

(*N,N*-Diallyldithiocarbamato- κ^2S,S')triphenyltin(IV) and bis(*N,N*-diallyldithiocarbamato- κ^2S,S')-diphenyltin(IV): crystal structure, Hirshfeld surface analysis and computational study

Farah Natasha Haezam,^a Normah Awang,^{a‡} Nurul Farahana Kamaludin,^a Mukesh M. Jotani^b and Edward R. T. Tiekink^{c*}

Received 6 January 2020

Accepted 6 January 2020

Edited by W. T. A. Harrison, University of Aberdeen, Scotland

‡ Additional correspondence author, email: awang_normah@yahoo.com.

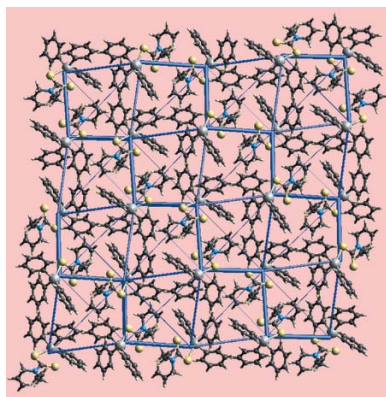
Keywords: crystal structure; organotin; dithiocarbamate; Hirshfeld surface analysis; computational chemistry.

CCDC references: 1975797; 1975796

Supporting information: this article has supporting information at journals.iucr.org/e

^aEnvironmental Health and Industrial Safety Programme, Faculty of Health Sciences, Universiti Kebangsaan Malaysia, Jalan Raja Muda Abdul Aziz, 50300 Kuala Lumpur, Malaysia, ^bDepartment of Physics, Bhavan's Sheth R. A. College of Science, Ahmedabad, Gujarat 380001, India, and ^cResearch Centre for Crystalline Materials, School of Science and Technology, Sunway University, 47500 Bandar Sunway, Selangor Darul Ehsan, Malaysia. *Correspondence e-mail: edwardt@sunway.edu.my

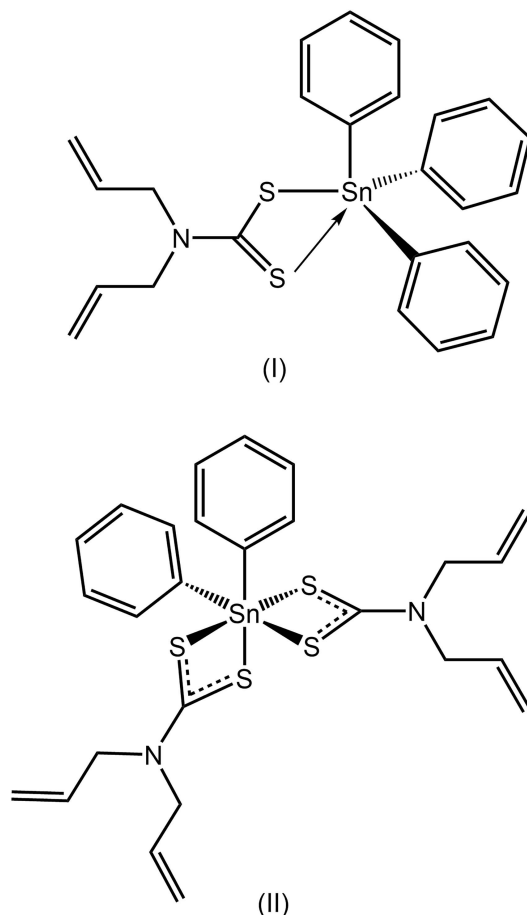
The crystal and molecular structures of the title organotin dithiocarbamate compounds, [Sn(C₆H₅)₃(C₇H₁₀NS₂)] (I) and [Sn(C₆H₅)₂(C₇H₁₀NS₂)₂] (II), present very distinct tin atom coordination geometries. In (I), the dithiocarbamate ligand is asymmetrically coordinating with the resulting C₃S₂ donor set defining a coordination geometry intermediate between square-pyramidal and trigonal-bipyramidal. In (II), two independent molecules comprise the asymmetric unit, which differ in the conformations of the allyl substituents and in the relative orientations of the tin-bound phenyl rings. The dithiocarbamate ligands in (II) coordinate in an asymmetric mode but the Sn–S bonds are more symmetric than observed in (I). The resulting C₂S₄ donor set approximates an octahedral coordination geometry with a *cis*-disposition of the *ipso*-carbon atoms and with the more tightly bound sulfur atoms approximately *trans*. The only directional intermolecular contacts in the crystals of (I) and (II) are of the type phenyl-C–H··· π (phenyl) and vinylidene-C–H··· π (phenyl), respectively, with each leading to a supramolecular chain propagating along the *a*-axis direction. The calculated Hirshfeld surfaces emphasize the importance of H···H contacts in the crystal of (I), *i.e.* contributing 62.2% to the overall surface. The only other two significant contacts also involve hydrogen, *i.e.* C···H/H···C (28.4%) and S···H/H···S (8.6%). Similar observations pertain to the individual molecules of (II), which are clearly distinguishable in their surface contacts, with H···H being clearly dominant (59.9 and 64.9%, respectively) along with C···H/H···C (24.3 and 20.1%) and S···H/H···S (14.4 and 13.6%) contacts. The calculations of energies of interaction suggest dispersive forces make a significant contribution to the stabilization of the crystals. The exception is for the C–H··· π contacts in (II) where, in addition to the dispersive contribution, significant contributions are made by the electrostatic forces.



1. Chemical context

Dithiocarbamate anions of general formula [−]S₂CNRR', R/R' = H, alkyl and aryl, are readily prepared from the facile reaction of an amine with CS₂ in the presence of base. Thus, the number of derivatives which can be prepared is largely dictated by the availability of amines and hence, an enormous range of dithiocarbamate anions are available for complexation to metals/heavy elements. A key interest in developing metal/heavy element compounds of dithiocarbamates relates to their biological potential (Hogarth, 2012). In the context of

anti-cancer properties, a number of recent reports have described the efficacy of phosphane-gold (Jamaludin *et al.*, 2013), zinc (Tan *et al.*, 2015) and bismuth (Ishak *et al.*, 2014) dithiocarbamates, buoyed by the observation that many of these species promote cancer cell death by apoptosis; bismuth derivatives exhibit *in vivo* anti-tumour activity (Li *et al.*, 2007). Organotin compounds are well known for their anti-cancer potential (Gielen & Tiekink, 2005) and there is a strong body of literature on organotin dithiocarbamates in this context (Tiekink, 2008).



In the past few years, there has been a resurgence of interest in the anti-cancer activity of organotin dithiocarbamates (Khan *et al.*, 2015; Mohamad, Awang, Kamaludin *et al.*, 2016) and very recently, a report on the *in vitro* cytotoxicity trial of several tin diallyldithiocarbamate compounds was described as well as a preliminary assessment of anti-microbial activity (Adeyemi *et al.*, 2019); some phosphane-gold(I) and phosphane-silver(I) dithiocarbamates are known to be bactericidal based on pharmacokinetic studies (Sim *et al.*, 2014; Tan, Tan *et al.*, 2019). The aforementioned report on tin diallyldithiocarbamate compounds (Adeyemi *et al.*, 2019) also presented the first crystal-structure determinations for tin compounds of diallyldithiocarbamate. In a continuation of recent structural studies in this area (Mohamad *et al.*, 2017, 2018*a,b*; Haezam *et al.*, 2019), herein, two organotin compounds of diallyldithiocarbamate, $(\text{C}_6\text{H}_5)_3\text{Sn}[\text{S}_2\text{CN}(\text{CH}_2\text{C}(\text{H})=\text{CH}_2)_2]$, (I), and $(\text{C}_6\text{H}_5)_2\text{Sn}[\text{S}_2\text{CN}(\text{CH}_2\text{C}(\text{H})=\text{CH}_2)_2]_2$, (II), have been synth-

Table 1
Selected geometric parameters (\AA , $^\circ$) for (I).

Parameter	(I)	Parameter	(I)
Sn—S1	2.4749 (4)	Sn—S2	2.9456 (5)
Sn—C11	2.1427 (19)	Sn—C21	2.130 (2)
Sn—C31	2.1673 (19)	C1—S1	1.7559 (19)
C1—S2	1.6894 (19)	C1—N1	1.330 (3)
S1—Sn—S2	65.470 (14)	C11—Sn—C21	111.15 (7)
C11—Sn—C31	104.14 (7)	C21—Sn—C31	107.13 (7)
S1—Sn—C11	128.76 (5)	S2—Sn—C31	156.01 (5)

esized and studied by X-ray crystallography. In addition, the supramolecular associations in their crystals have been evaluated by Hirshfeld surface analyses and computational chemistry.

2. Structural commentary

The tin atom in (I), Fig. 1, is coordinated by three *ipso*-carbon atoms of the phenyl groups as well as by an asymmetrically bound dithiocarbamate anion, Table 1. There is a relatively large disparity in the Sn—S separations, *i.e.* $\Delta(\text{Sn—S}) = [(\text{Sn—S}_{\text{long}}) - (\text{Sn—S}_{\text{short}})] = 0.47 \text{ \AA}$, indicating that the Sn—S2 interaction is weak. Evidence in support of this conclusion is seen in the pattern of C—S bond lengths. Thus, the C1—S2 bond involving the less tightly bound S2 atom is about 0.07 \AA shorter than the analogous bond with the tightly bound S1 atom. Nevertheless, there is a clear influence exerted by the S2 atom upon the Sn—C bond lengths with the Sn—C31 bond being appreciably longer than the other Sn—C bonds. This is traced to the *trans* effect exerted by the S2 atom as this forms a S2—Sn—C31 angle $156.01 (5)^\circ$. It is noted that there is no other (approximate) *trans* angle subtended at the tin atom in (I). Assuming a five-coordinate, C_3S_2 , geometry, the range of

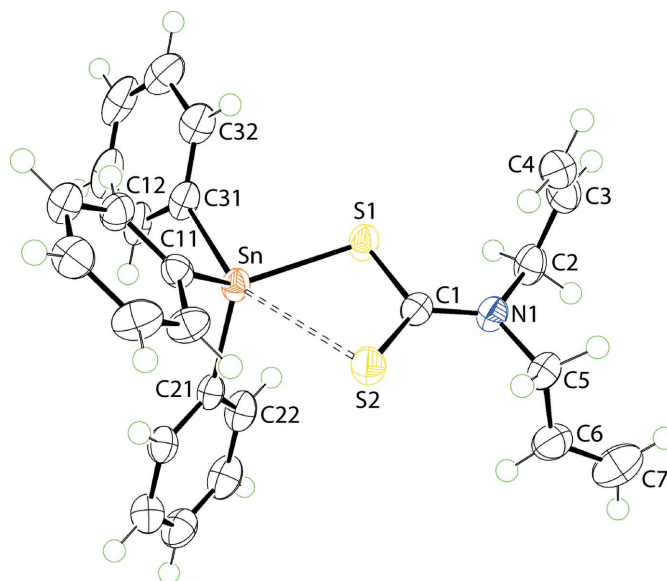


Figure 1
The molecular structure of (I) showing the atom-labelling scheme and displacement ellipsoids at the 70% probability level.

angles subtended at the tin atom is $65.470(14)^\circ$, for the S1—Sn—S2 chelate angle, to the aforementioned *trans* angle. The value of τ is a convenient descriptor for the assignment of a five-coordinate geometry, which ranges in value from 0.0 for an ideal square pyramid to 1.0 for an ideal trigonal bipyramid (Addison *et al.*, 1984). The value of τ the case of (I) is 0.45, which is indicative of an intermediate geometry with a slight tendency towards square pyramidal. On the other hand, should the coordination geometry be considered C_3S tetrahedral, *i.e.* the weak Sn—S2 bond was ignored, the range of tetrahedral angles would be $91.01(5)^\circ$, for S1—Sn—C31, to $128.76(5)^\circ$, for S1—Sn—C11. Finally, it is noted the C1—N1 bond length of $1.330(3) \text{ \AA}$ is consistent with significant double-bond character in this bond, which arises from a major contribution of the ${}^2\text{-S}_2\text{C}=\text{N}^+(\text{CH}_2\text{C}(\text{H})=\text{CH}_2)_2$ canonical form to the electronic structure of the dithiocarbamate ligand.

A distinct coordination geometry for the tin atoms is noted for (II), Fig. 2, for which two independent molecules comprise the crystallographic asymmetric unit. The tin atom in each

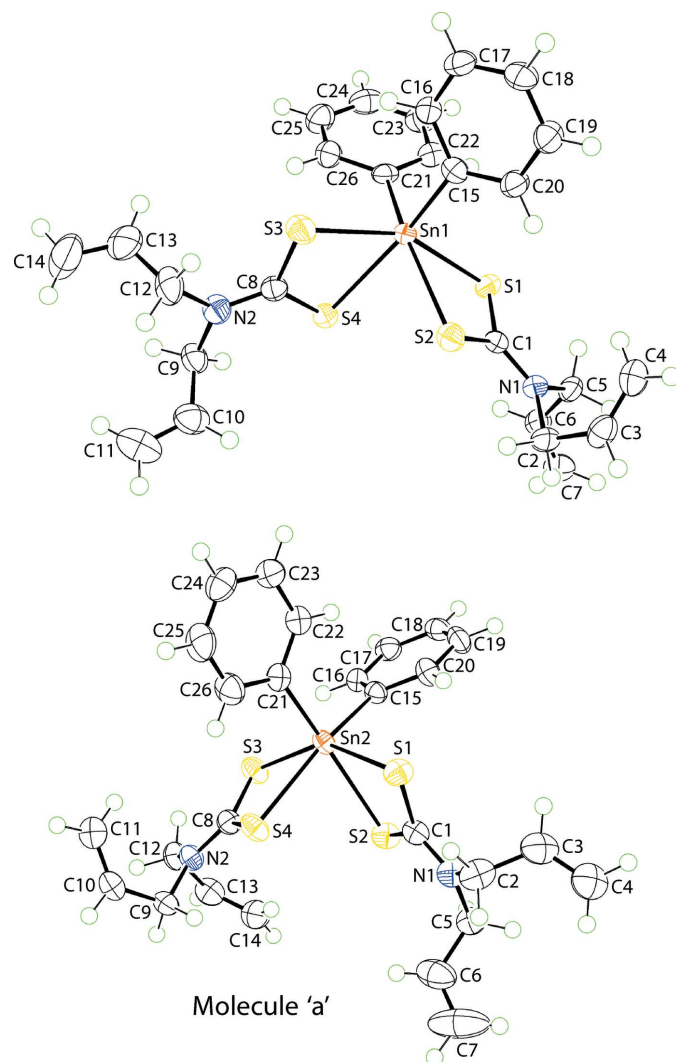


Figure 2
The molecular structures of the two independent molecules comprising the asymmetric unit of (II) showing the atom-labelling scheme and displacement ellipsoids at the 70% probability level.

Table 2
Selected geometric parameters (\AA , $^\circ$) for the two independent molecules in (II).

Parameter	Sn1-molecule	Sn2-molecule
Sn—S1	2.5501 (6)	2.5585 (7)
Sn—S2	2.7393 (7)	2.7664 (7)
Sn—S3	2.5726 (7)	2.5700 (6)
Sn—S4	2.6754 (6)	2.6750 (6)
C1—S1	1.742 (3)	1.740 (3)
C1—S2	1.710 (3)	1.704 (3)
C8—S3	1.738 (3)	1.733 (3)
C8—S4	1.715 (3)	1.716 (3)
C1—N1	1.326 (3)	1.328 (4)
C8—N2	1.318 (3)	1.327 (3)
S1—Sn—S2	67.824 (19)	67.18 (2)
S3—Sn—S4	67.97 (2)	68.69 (2)
S1—Sn—S3	154.38 (2)	149.00 (2)
S2—Sn—C21	159.42 (7)	161.40 (7)
S4—Sn—C15	160.59 (7)	159.91 (7)
C15—Sn—C21	99.84 (9)	103.34 (9)
N1—C2—C3—C4	12.5 (4)	9.9 (4) ^a
N1—C5—C6—C7	−122.3 (3)	13.3 (4) ^a
N2—C9—C10—C11	105.3 (3)	105.2 (3) ^a
N2—C12—C13—C14	110.9 (4)	114.6 (4) ^a

Note: (a) for ease of comparison, the torsion angles are for the inverted Sn2-molecule.

molecule is coordinated by two *ipso*-carbon atoms of the phenyl groups as well as by two asymmetrically bound dithiocarbamate anions, Table 2. There is a disparity in the Sn—S separations, *i.e.* $\Delta(\text{Sn—S}) = 0.19$ and 0.11 \AA , for the S1- and S3-dithiocarbamate anions of the first independent molecule; the comparable values for the second molecule are similar at 0.21 and 0.11 \AA . The disparities in $\Delta(\text{Sn—S})$ are reflected in the associated C—S bond distances, Table 2. Gratifyingly, the greater differences in C—S bonds, *i.e.* 0.03 and 0.04 \AA for the S1-dithiocarbamate anions of each independent molecule, are correlated with the greater values in $\Delta(\text{Sn—S})$. The C1—N1 and C8—N2 bond lengths in both molecules are short for the reasons mentioned for (I) above. The C_2S_4 coordination geometry is based on an octahedron and has a *cis*-disposition of the *ipso*-carbon atoms with the more tightly bound sulfur atoms close to being *trans*. A partial explanation of the lengthening of the Sn—S2 and Sn—S4 bonds relates to the *trans*-influence exerted by the phenyl substituents approximately opposite the S2 and S4 atoms.

A view of the superimposition of the two molecules comprising the asymmetric unit in (II) is shown in Fig. 3 whereby the Sn1- and inverted-Sn2-molecules are overlapped so that two chelate rings, *i.e.* (Sn1,S1,S2,C1) and (Sn2,S3,S4,C8), are coincident. This shows there are non-trivial conformational differences between the molecules. While the dihedral angles between the two phenyl substituents are equal within experimental error in the two molecules, *i.e.* $81.28(13)$ and $81.63(14)^\circ$, more telling are the angles they form with the respective, *cis*-disposed chelate rings, *i.e.* $81.06(10)$ and $35.93(10)^\circ$ for the Sn1-molecule and $15.35(11)$ and $74.71(6)^\circ$ for the Sn2-molecule. Differences are also noted in the relative orientations of the allyl substituents. Thus, for the overlapped dithiocarbamate ligands, the N1—

Table 3

Hydrogen-bond geometry (Å, °) for (I).

$Cg1$ and $Cg2$ are the centroids of the (C21–C26) and (C31–C36) rings, respectively.

$D-H\cdots A$	$D-H$	$H\cdots A$	$D\cdots A$	$D-H\cdots A$
C13–H13 $\cdots Cg1^i$	0.95	2.92	3.605 (2)	130
C23–H23 $\cdots Cg2^{ii}$	0.95	2.99	3.720 (3)	134

Symmetry codes: (i) $x - 1, y, z$; (ii) $x + 1, y, z$.

C5–C6–C7 torsion angle of $-122.3 (3)^\circ$ is an outlier with respect to the other torsion angles with the direct equivalent angle for the inverted Sn2-molecule being $13.3 (4)^\circ$. While the N–C–C–C torsion angles for the second pair of dithiocarbamate ligands are similar, Table 2, there is a misalignment of these ligands as seen in the dihedral angle formed between the chelate rings of $80.98 (5)$ and $76.55 (6)^\circ$ for the Sn1- and Sn2-molecules, respectively.

The difference in coordination modes of the dithiocarbamate ligands and coordination geometries are related, at least in part, to the different Lewis acid strength of the tin atoms, with the Lewis acidity in the triphenyltin species being significantly less than that in the diphenyltin species.

3. Supramolecular features

The only directional point of contact between molecules based on the distance criteria in *PLATON* (Spek, 2020) are phenyl-C–H $\cdots\pi$ (phenyl) interactions, Table 3. Here, the (C21–C26) ring is pivotal by donating a C–H atom to a symmetry-related

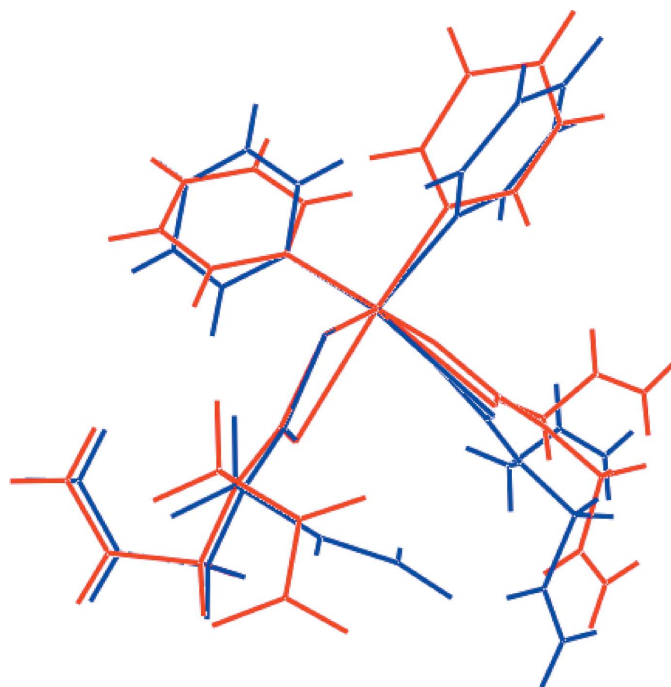


Figure 3

Overlay diagram of the independent molecules comprising the asymmetric unit of (II): (a) Sn1-containing molecule (red image) and (b) inverted-Sn2-molecule (blue). The molecules are overlapped so that the (Sn1,S1,S2,C1) and (Sn2,S3,S4,C8) residues are coincident.

Table 4

Hydrogen-bond geometry (Å, °) for (II).

$Cg1$ and $Cg2$ are the centroids of the (C15A–C20A) and (C21A–C26A) rings, respectively.

$D-H\cdots A$	$D-H$	$H\cdots A$	$D\cdots A$	$D-H\cdots A$
C7–H7A $\cdots Cg1^i$	0.95	2.83	3.774 (3)	172
C7–H7B $\cdots Cg2^{ii}$	0.95	2.92	3.582 (3)	128

Symmetry codes: (i) $-x + 2, -y + 1, -z + 1$; (ii) $-x + 1, -y + 1, -z + 1$.

(C31–C36) ring and the same time accepting a phenyl-C–H $\cdots\pi$ (phenyl) interaction from a (C11–C16) ring to construct a linear, supramolecular chain aligned along the a -axis direction, Fig. 4(a). The chains assemble in the crystal without directional interactions between them, Fig. 4(b).

The molecular packing in (II) is also largely devoid of directional interactions. Indeed, the only connections evident are vinylidene-C–H $\cdots\pi$ (phenyl) interactions, Table 4, which serve to link the independent molecules comprising the asymmetric unit into a supramolecular chain aligned along the a -axis direction. In essence, the vinylidene-hydrogen atoms of the Sn1-molecule bridge translationally related Sn2-molecules into a linear chain, Fig. 5(a). The chains pack without directional interactions between them, Fig. 5(b).

4. Hirshfeld surface analysis

In order to gain further insight into the molecular packing of each of (I) and (II), Hirshfeld surface calculations were

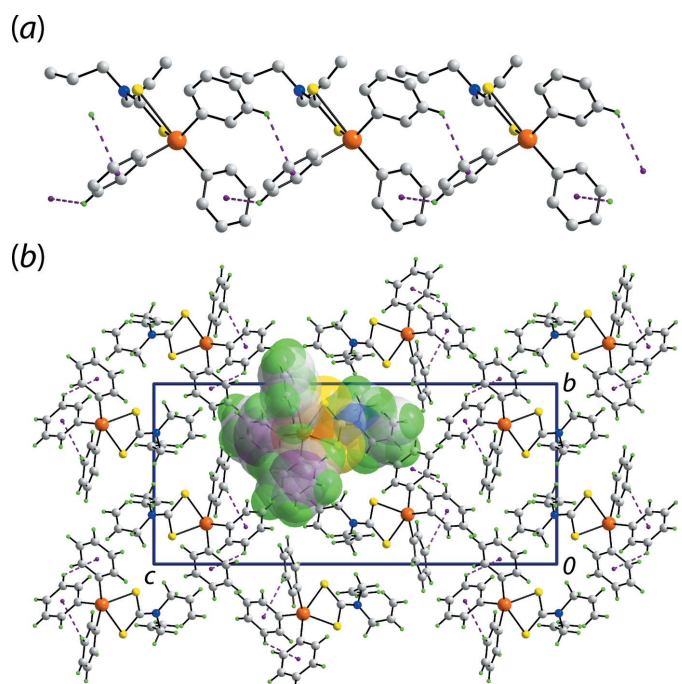


Figure 4

Molecular packing in the crystal of (I): (a) supramolecular chain along the a -axis direction sustained by phenyl-C–H $\cdots\pi$ (phenyl) interactions shown as purple dashed lines (non-participating hydrogen atoms have been removed) and (b) a view of the unit-cell contents in projection down the a axis with one chain highlighted in space-filling mode.

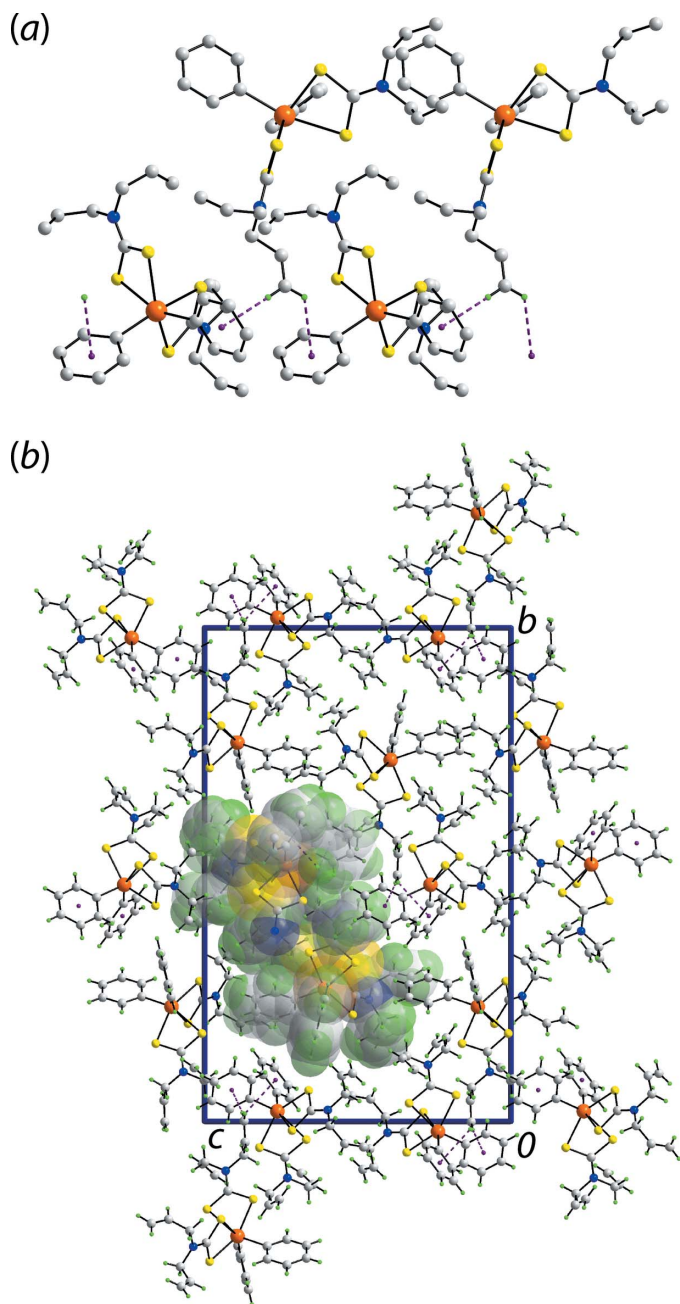


Figure 5
Molecular packing in the crystal of (II): (a) supramolecular chain along the *a*-axis direction sustained by methylene-C–H \cdots π (phenyl) interactions shown as purple dashed lines (non-participating hydrogen atoms have been removed) and (b) a view of the unit-cell contents in projection down the *a* axis with one chain highlighted in space-filling mode.

performed with *Crystal Explorer 17* (Turner *et al.*, 2017) following literature protocols (Tan, Jotani *et al.*, 2019). The calculations highlight the influence of the discussed C–H \cdots π interactions (Tables 3 and 4) as well as the short interatomic contacts collated in Table 5. The short interatomic contacts are indicated as diminutive or faint-red spots near the participating atoms on the Hirshfeld surfaces mapped over d_{norm} for (I) and (II) in Figs. 6 and 7, respectively. Further, the donors and acceptors of the intermolecular C–H \cdots π contacts for

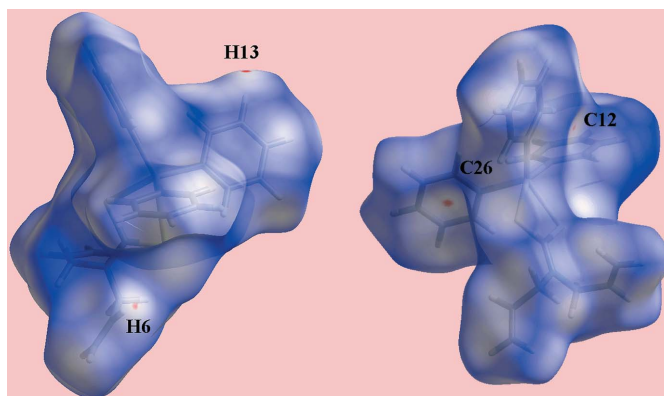


Figure 6
Two views of Hirshfeld surface for (I) mapped over d_{norm} in the range -0.028 to $+1.257$ arbitrary units.

both (I) and (II) are evident as the blue bumps and red concave regions, respectively, on the Hirshfeld surfaces mapped with shape-index property shown in Fig. 8. In the absence of potential hydrogen bonds in (I) and (II), both the blue and red regions corresponding to positive and negative electrostatic potential, respectively, on Hirshfeld surfaces mapped over electrostatic potential in Fig. 9 and arise owing to the polarization of charges towards the participating residues.

The overall two-dimensional fingerprint plots for (I) and the individual molecules of (II) are illustrated in Fig. 10(a), and those delineated into H \cdots H, C \cdots H/H \cdots C and S \cdots H/H \cdots S contacts are illustrated in Fig. 10(b)–(d), respectively. The percentage contributions from different atom–atom contacts to the Hirshfeld surfaces of (I), Sn1- and Sn2-molecules of (II) are quantitatively summarized in Table 6. In the fingerprint

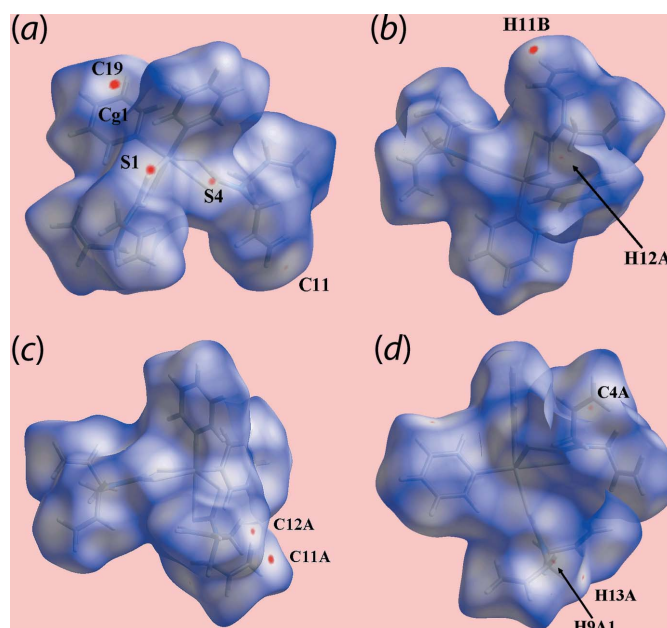


Figure 7
Views of the Hirshfeld surfaces for (II) mapped over d_{norm} for the (a) and (b) Sn1-molecule in the range -0.026 to $+1.372$ arbitrary units, and (c) and (d) Sn2-molecule in the range -0.027 to $+1.383$ arbitrary units.

Table 5
Summary of short interatomic contacts (Å) in (I) and (II)^a.

Contact	Distance	Symmetry operation
(I)		
C12...H6	2.76	$-1 + x, y, z$
C16...H5B	2.80	$1 - x, -y, 1 - z$
C25...H4B	2.78	$x, \frac{1}{2} - y, -\frac{1}{2} + z$
C26...H13	2.74	$1 + x, y, z$
C33...H2B	2.79	$1 - x, 1 - y, 1 - z$
H15...H24	2.19	$1 - x, -\frac{1}{2} + y, \frac{1}{2} - z$
S1...H7B	2.91	$-1 + x, y, z$
S1...H2A	2.96	$1 - x, 1 - y, 1 - z$
(II)		
S1...C11A	3.455 (3)	$1 - x, 1 - y, 1 - z$
S4...C12A	3.473 (3)	$1 - x, 1 - y, 1 - z$
C11...C23A	3.386 (5)	x, y, z
C11...H23A	2.81	x, y, z
C19...H11B	2.71	$1 + x, \frac{1}{2} - y, \frac{1}{2} + z$
C21...H12D	2.78	$1 - x, 1 - y, 1 - z$
H12A...H9A2	2.16	$1 - x, -\frac{1}{2} + y, \frac{1}{2} - z$
H17...H26	2.18	$1 + x, y, z$
C4A...H9A1	2.75	$1 - x, 1 - y, -z$
S1A...H18	2.91	$1 - x, \frac{1}{2} - y, -\frac{1}{2} + z$
H17...H13A	2.33	$2 - x, 1 - y, 1 - z$

Note: (a) The interatomic distances are calculated in *Crystal Explorer 17* (Turner *et al.*, 2017) whereby the X–H bond lengths are adjusted to their neutron values.

plot delineated into H...H contacts for (I), Fig. 10(b), a pair of small and proximate peaks at $d_e + d_i \sim 2.2$ Å results from the presence of a short interatomic contact between the phenyl-H15 and H24 atoms, Table 5. The presence of a single peak at $d_e + d_i \sim 2.2$ Å in the analogous plot for the Sn1-molecule of (II) is due to the short H...H contact between the phenyl-H17 and H26 atoms. Another short interatomic H...H contact

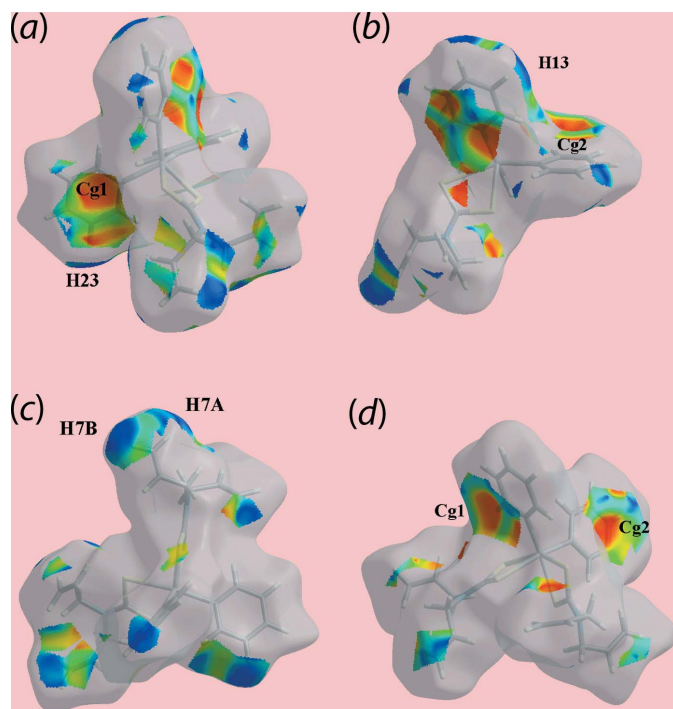


Figure 8
Views of Hirshfeld surfaces mapped with the shape-index property highlighting donors and acceptors of the intermolecular C–H... π contacts for (a) and (b) (I), and (c) and (d) (II).

Table 6
Percentage contributions of interatomic contacts to the Hirshfeld surface for (I), the Sn1-molecule in (II) and the Sn2-molecule in (II).

Contact	Percentage contribution		
	(I)	Sn1-molecule in (II)	Sn2-molecule in (II)
H...H	62.2	59.9	64.9
C...H/H...C	28.4	24.3	20.1
S...H/H...S	8.6	14.4	13.6
N...H/H...N	0.1	0.8	0.7
C...C	0.4	0.3	0.1
S...C/C...S	0.2	0.4	0.6
Sn...H/H...Sn	0.1	0.0	0.0

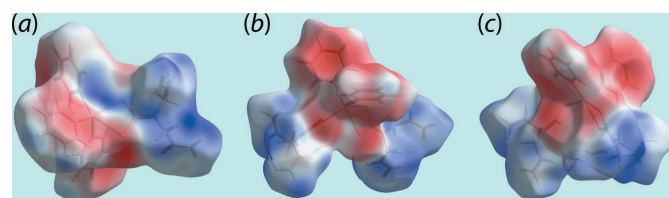


Figure 9
Views of Hirshfeld surfaces mapped over the electrostatic potential (the red and blue regions represent negative and positive electrostatic potentials, respectively) for (a) (I) in the range -0.032 to $+0.043$ atomic units (a.u.), (b) the Sn1-molecule in (II) in the range -0.039 to $+0.040$ a.u. and (c) the Sn2-molecule in (II) in the range -0.038 to $+0.047$ a.u.

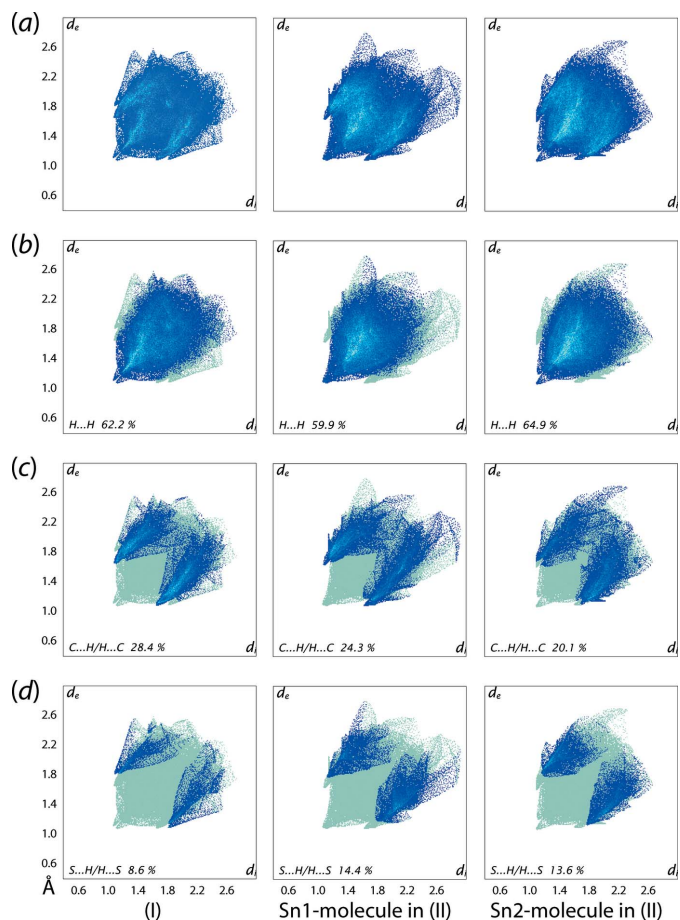


Figure 10
(a) A comparison of the full two-dimensional fingerprint plot for (I) and for the Sn1- and Sn2-molecules of (II), and those delineated into (b) H...H, (c) C...H/H...C and (d) S...H/H...S contacts.

Table 7
Summary of interaction energies (kJ mol⁻¹) calculated for (I) and (II).

Contact	<i>R</i> (Å)	<i>E</i> _{ele}	<i>E</i> _{pol}	<i>E</i> _{dis}	<i>E</i> _{rep}	<i>E</i> _{tot}
(I)^a						
H13...C26 ⁱ + C13–H13...C _g (C21–C26) ⁱ + C23–H23...C _g (C31–C36) ⁱ + H6...C12 ⁱ + H7B...S1 ⁱ	8.06	-13.8	-5.6	-68.5	42.5	-45.0
C16...H5B ⁱⁱ	8.42	-21.8	-5.6	-52.2	29.1	-49.3
C33...H2B ⁱⁱⁱ + S1...H2A ⁱⁱⁱ	8.00	-21.2	-7.0	-59.2	29.5	-55.6
C25...H4B ^{iv}	9.91	-0.6	-0.8	-23.3	8.4	-15.2
H15...H24 ^v	12.94	-2.6	-0.5	-12.5	9.1	-6.9
(II)^b						
S1...C11A ⁱ + S4...C12A ⁱ + C7–H7B...C _g (C21A–C26A) ⁱ + C21...H12D ⁱ	8.68	-25.4	-8.6	-67.8	44.0	-57.0
C4A...H9A1 ⁱⁱ	9.0	-28.8	-7.3	-69.0	49.0	-56.5
C7–H7A...C _g (C15A–C20A) ⁱⁱⁱ + H17...H13A ⁱⁱⁱ	9.21	-19.6	-7.4	-61.3	33.7	-52.6
H17...H26 ^{iv}	9.62	-12.0	-5.0	-51.2	25.9	-40.6
C11...C23A ^v	9.93	-10.2	-2.9	-44.1	23.5	-33.0
C11...H23A ^v						
H12A...H9A2 ^{vi}	10.81	-5.9	-2.4	-30.6	14.5	-23.4
S1A...H18 ^{vii}	10.11	-5.2	-3.6	-34.3	18.9	-23.0
C19...H11B ^{viii}	12.51	-7.4	-2.6	-20.5	9.8	-19.8

Notes: (a) Symmetry operations for (I): (i) $-1 + x, y, z$; (ii) $1 - x, -y, 1 - z$; (iii) $1 - x, 1 - y, 1 - z$; (iv) $x\frac{1}{2} - y, -\frac{1}{2} + z$; (v) $1 - x, -\frac{1}{2} + y, \frac{1}{2} - z$. (b) Symmetry operations for (II): (i) $1 - x, 1 - y, 1 - z$; (ii) $1 - x, 1 - y, -z$; (iii) $2 - x, 1 - y, 1 - z$; (iv) $1 + x, y, z$; (v) x, y, z ; (vi) $1 - x, -\frac{1}{2} + y, \frac{1}{2} - z$; (vii) $1 - x, \frac{1}{2} - y, -\frac{1}{2} + z$; (viii) $1 + x, \frac{1}{2} - y, \frac{1}{2} + z$.

involving the H17 and H18A atoms of the Sn1-molecule and the H9A2 and H13A atoms of the Sn2-molecule, Table 5, are evident as the pair of peaks at $d_e + d_i \sim 2.2$ Å and at $d_e + d_i \sim 2.3$ Å in the corresponding delineated plot for the Sn2-molecule.

The presence of short interatomic C...H/H...C contacts in each of (I) and (II), summarized in Table 5, are evident as the forceps-like tips at $d_e + d_i \sim 2.8$ Å in Fig. 10(a). Also, the intermolecular C–H...π contacts are characterized as a pair of wings in their respective delineated plots shown in Fig. 10(c). The short interatomic C...H/H...C contacts in the crystal of (II) appear as a pair of forceps-like tips at $d_e + d_i \sim 2.7$ Å for the Sn1-molecule and as two pairs of similar adjoining tips at the same distances $d_e + d_i \sim 2.8$ Å for the Sn2-molecule in the plots of Fig. 10(c). For (I), in the fingerprint plot delineated into S...H/H...S contacts of Fig. 10(d), the short interatomic contacts involving thiocarbamate-S1 and the H2A and H7B atoms are evident as the pair of conical tips at $d_e + d_i \sim 2.9$ Å. Similar contacts in the crystal of (II) are also evident as the conical tips at $d_e + d_i \sim 2.9$ Å in Fig. 10(d) in the upper and lower regions of the plots for the Sn1- and Sn2-molecules, respectively.

5. Computational chemistry

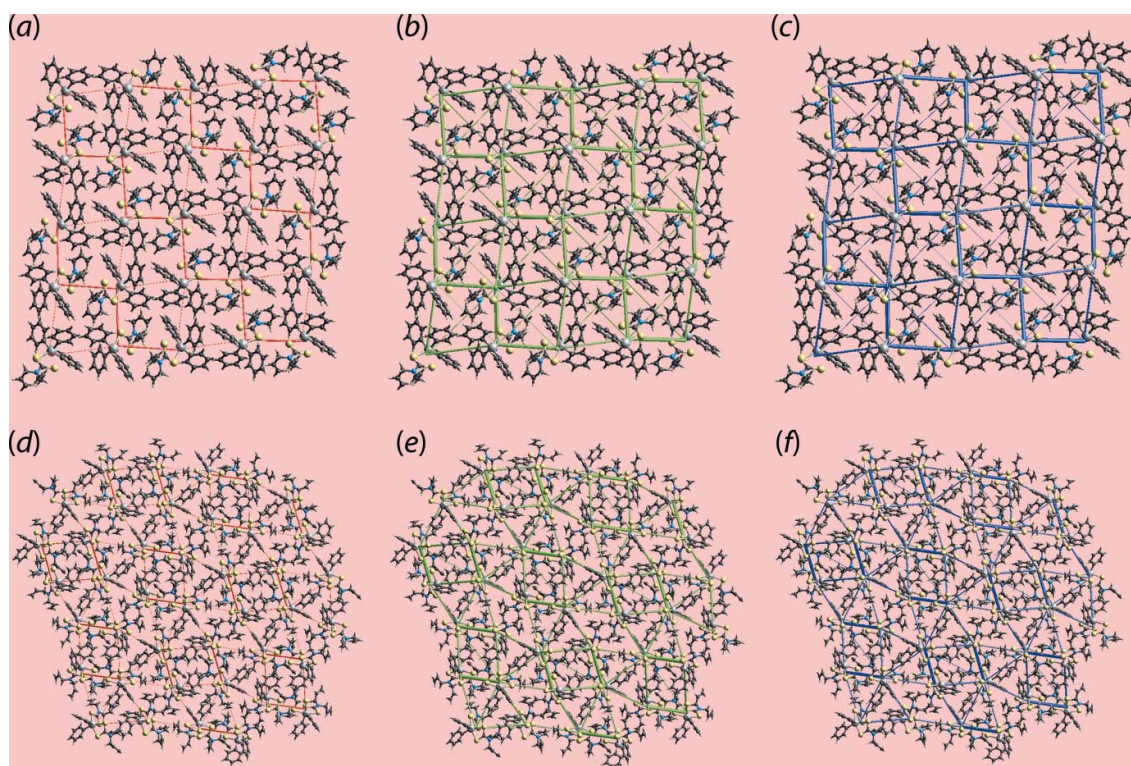
The pairwise interaction energies between the molecules within the crystals of (I) and (II) were calculated by summing up four energy components, namely the electrostatic (E_{ele}), polarization (E_{pol}), dispersion (E_{dis}) and exchange-repulsion (E_{rep}) energies, in accord with literature protocols (Turner *et*

al., 2017). In the present analysis, these energies were obtained by using the wave function calculated at the HF/3-21G level of theory. The specific contacts and associated energies are quantitatively summarized in Table 7. An analysis of these energies for (I) and (II) reveals that the dispersive component makes the major contribution to all the specified intermolecular interactions in the crystals of (I) and (II). However, as clearly evident from the relevant interaction energies listed in Table 7 and in the Hirshfeld surfaces mapped over the electrostatic potential of Fig. 9, where intense blue and red regions are apparent around the donors and acceptors, the C–H...π contacts in (II) have more significant contributions from the E_{ele} component, in contrast to mainly dispersive contributions in the case of (I).

A further noticeable observation about the strength of the intermolecular interactions from Table 7 is that those intermolecular contacts arising from the same pair of symmetry-related molecules have the greater interaction energies. The magnitudes of intermolecular energies were also represented graphically by energy frameworks to view the supramolecular architecture of both the crystals through cylinders joining the centroids of molecular pairs using red, green and blue colour codes for the E_{ele} , E_{disp} and E_{tot} terms, respectively. In summary, the images of Fig. 11 highlight the importance of dispersion forces in the crystals of (I) and (II).

6. Database survey

As a result of having several important applications, such as biological activity as alluded to in the *Chemical Context*, a


Figure 11

The energy frameworks calculated for (I) viewed down the a -axis direction showing the (a) electrostatic potential force, (b) dispersion force and (c) total energy. The corresponding plots for (II), viewed down the a -axis direction are shown in (d)–(f), respectively. The energy frameworks were adjusted to the same scale factor of 50 with a cut-off value of 5 kJ mol^{-1} within $2 \times 2 \times 2$ unit cells.

relatively large number of organotin dithiocarbamates have been synthesized and investigated by X-ray crystallography (Tiekink, 2008). The coordination geometry described for (I) conforms with literature expectations in that all $R_3\text{Sn}(\text{S}_2\text{CNR}'R'')$ molecules conform to this structural motif (Tiekink, 2008; Mohamad *et al.*, 2018a). The Sn–S1 bond length in (I) of 2.4749 (4) Å is slightly longer than the average Sn–S_{short} bond of 2.47 Å in all $\text{Ph}_3\text{Sn}(\text{S}_2\text{CNR}'R'')$ structures, while the Sn–S2 bond of 2.9456 (5) Å in (I) is about 0.10 Å shorter than the average Sn–S_{long} of 3.04 Å in these structures. Consistent with these trends, $\Delta(\text{Sn}–\text{S})$ in (I) of 0.47 Å is less than the average $\Delta(\text{Sn}–\text{S})$ value of 0.57 Å calculated from all $\text{Ph}_3\text{Sn}(\text{S}_2\text{CNR}'R'')$ structures.

Greater structural diversity is noted for $R_2\text{Sn}(\text{S}_2\text{CNR}'R'')$ (Tiekink, 2008), including differences in coordination numbers and geometries (Mohamad, Awang, Jotani *et al.*, 2016). Of the now, 17 structures of the general formula $\text{Ph}_2\text{Sn}(\text{S}_2\text{CNR}'R'')$, nine adopt the *cis*- C_2S_4 structural motif exemplified by (II), including the two polymorphs of $\text{Ph}_2\text{Sn}(\text{S}_2\text{CNEt}_2)_2$ (Lindley & Carr, 1974; Hook *et al.*, 1994). The remaining structures adopt the usual motif for $R_2\text{Sn}(\text{S}_2\text{CNR}'R'')$, namely a geometry based on a bipyramidal skewed-bipyramid. Here, the dithiocarbamate ligands coordinate in an asymmetric fashion with the tin-bound phenyl substituents disposed to lie over the weaker Sn–S bonds, exemplified by the two independent molecules comprising the asymmetric unit of $\text{Ph}_2\text{Sn}[\text{S}_2\text{CN}(\text{Me})\text{Hex}]_2$ (Hex = *n*-hexyl, $-\text{C}_7\text{H}_{15}$) (Ramasamy *et al.*, 2013). Clearly there is a subtle interplay between the

electronic and steric characteristics of the dithiocarbamate ligands and molecular packing effects in determining the structural motif adopted by $\text{Ph}_2\text{Sn}(\text{S}_2\text{CNR}'R'')$ in their respective crystals.

7. Synthesis and crystallization

All chemicals and solvents were used as purchased without purification. The melting point was determined using an automated melting point apparatus (MPA 120 EZ-Melt). Carbon, hydrogen and nitrogen analyses were performed on a Leco CHNS-932 Elemental Analyzer.

The synthesis of (I) and (II) followed established literature procedures (Awang *et al.*, 2011; Ajibade *et al.*, 2011). For each synthesis, initially, diallylamine (Aldrich; 1.27 ml, 10 mmol) dissolved in ethanol (30 ml) was stirred under ice-bath conditions for 20 mins. A 25% ammonia solution (1 to 2 ml) was added followed by stirring for 30 mins to establish basic conditions. Then, a cold ethanolic solution of carbon disulfide (0.60 ml, 10 mmol) was added dropwise into the solution and stirred for about 2 h.

For (I), triphenyltin(IV) dichloride (Merck; 3.85 g, 10 mmol) dissolved in ethanol (20–30 ml) was added dropwise into the diallyldithiocarbamate solution and further stirred for 2 to 3 h. Next, the precipitate that formed was filtered off and washed with cold ethanol a few times to remove any impurities. Finally, the filtered precipitate was dried in a desiccator overnight. Recrystallization was carried out by dissolving the

Table 8
Experimental details.

	(I)	(II)
Crystal data		
Chemical formula	[Sn(C ₆ H ₅) ₃ (C ₇ H ₁₀ NS ₂)]	[Sn(C ₆ H ₅) ₂ (C ₇ H ₁₀ NS ₂) ₂]
M_r	522.27	617.45
Crystal system, space group	Monoclinic, $P2_1/c$	Monoclinic, $P2_1/c$
Temperature (K)	100	100
a, b, c (Å)	8.0650 (1), 11.4490 (1), 25.8775 (2)	9.6160 (1), 30.4216 (2), 19.1928 (1)
β (°)	98.282 (1)	100.019 (1)
V (Å ³)	2364.51 (4)	5528.93 (8)
Z	4	8
Radiation type	Cu $K\alpha$	Cu $K\alpha$
μ (mm ⁻¹)	10.32	10.30
Crystal size (mm)	0.13 × 0.10 × 0.04	0.19 × 0.14 × 0.07
Data collection		
Diffractometer	XtaLAB Synergy, Dualflex, AtlasS2	XtaLAB Synergy, Dualflex, AtlasS2
Absorption correction	Gaussian (<i>CrysAlis PRO</i> ; Rigaku OD, 2018)	Gaussian (<i>CrysAlis PRO</i> ; Rigaku OD, 2018)
T_{\min} , T_{\max}	0.807, 1.000	0.633, 1.000
No. of measured, independent and observed [$I > 2\sigma(I)$] reflections	55086, 4226, 4083	67735, 9876, 9370
R_{int}	0.044	0.037
$(\sin \theta/\lambda)_{\text{max}}$ (Å ⁻¹)	0.597	0.597
Refinement		
$R[F^2 > 2\sigma(F^2)]$, $wR(F^2)$, S	0.020, 0.053, 1.01	0.027, 0.068, 1.02
No. of reflections	4226	9876
No. of parameters	262	595
H-atom treatment	H-atom parameters constrained	H-atom parameters constrained
$\Delta\rho_{\text{max}}$, $\Delta\rho_{\text{min}}$ (e Å ⁻³)	0.82, -0.50	1.23, -0.73

Computer programs: *CrysAlis PRO* (Rigaku OD, 2018), *SHELXS* (Sheldrick, 2015a), *SHELXL2017/1* (Sheldrick, 2015b), *ORTEP-3 for Windows* (Farrugia, 2012), *DIAMOND* (Brandenburg, 2006) and *publCIF* (Westrip, 2010).

compound in a chloroform and ethanol solvent mixture (5 ml; 1:1 *v/v*), which was allowed to slowly evaporate at room temperature yielding colourless crystals. Yield: 44%. M.p. 454.8–456.2 K. Elemental analysis: calculated (%): C 57.51, H 4.79, N 2.68. Found (%): C 56.92, H 4.93, N 2.93.

Compound (II) was prepared and recrystallized as for (I) but, using diphenyltin(IV) dichloride (Merck; 1.72 g, 5 mmol) dissolved in ethanol (20–30 ml). Yield: 52%. M.p. 332.5–334.4 K. Elemental analysis: calculated (%): C 50.59, H 4.86, N 4.54. Found (%): C 50.20, H 4.80, N 4.20.

8. Refinement

Crystal data, data collection and structure refinement details are summarized in Table 8. Carbon-bound H atoms were placed in calculated positions (C–H = 0.95–0.99 Å) and were included in the refinement in the riding-model approximation, with $U_{\text{iso}}(\text{H})$ set to 1.2 $U_{\text{eq}}(\text{C})$. In (II), the maximum and minimum residual electron density peaks of 1.23 and 0.73 e Å⁻³, respectively, were located 0.80 and 0.74 Å from the S2 and Sn1 atoms, respectively.

Acknowledgements

The authors gratefully acknowledge the Faculty of Health Sciences and the Faculty of Science and Technology of the Universiti Kebangsaan Malaysia for providing essential laboratory facilities and for technical support from the

laboratory assistants. The Universiti Teknologi MARA Puncak Alam is thanked for the elemental analysis.

Funding information

This work was supported by the Fundamental Research Grant Scheme (FRGS/1/2018/STG01/UKM/02/20) awarded by the Ministry of Education (MOE). Crystallographic research at Sunway University is supported by Sunway University Sdn Bhd (Grant no. STR-RCTR-RCCM-001-2019).

References

- Addison, A. W., Rao, T. N., Reedijk, J., van Rijn, J. & Verschoor, G. C. (1984). *J. Chem. Soc. Dalton Trans.* pp. 1349–1356.
- Adeyemi, J. O., Onwudiwe, D. C., Ekennia, A. C., Anokwuru, C. P., Nundkumar, N., Singh, M. & Hosten, E. C. (2019). *Inorg. Chim. Acta*, **485**, 64–72.
- Ajibade, P. A., Onwudiwe, D. C. & Moloto, M. J. (2011). *Polyhedron*, **30**, 246–252.
- Awang, N., Baba, I., Yamin, B. M., Othman, M. S. & Kamaludin, N. F. (2011). *Am. J. Appl. Sci.* **8**, 310–317.
- Brandenburg, K. (2006). *DIAMOND*. Crystal Impact GbR, Bonn, Germany.
- Farrugia, L. J. (2012). *J. Appl. Cryst.* **45**, 849–854.
- Gielen, M. & Tiekink, E. R. T. (2005). *Metallotherapeutic drugs and metal-based diagnostic agents: the use of metals in medicine*, edited by M. Gielen & E. R. T. Tiekink, pp. 421–439. Chichester: John Wiley & Sons Ltd.
- Haезam, F. N., Awang, N., Kamaludin, N. F., Jotani, M. M. & Tiekink, E. R. T. (2019). *Acta Cryst.* **E75**, 1479–1485.
- Hogarth, G. (2012). *Mini Rev. Med. Chem.* **12**, 1202–1215.

- Hook, J. M., Linahan, B. M., Taylor, R. L., Tiekink, E. R. T., Gorkom, L. & Webster, L. K. (1994). *Main Group Met. Chem.* **17**, 293–311.
- Ishak, D. H. A., Ooi, K. K., Ang, K. P., Akim, A. M., Cheah, Y. K., Nordin, N., Halim, S. N. B. A., Seng, H.-L. & Tiekink, E. R. T. (2014). *J. Inorg. Biochem.* **130**, 38–51.
- Jamaludin, N. S., Goh, Z.-J., Cheah, Y. K., Ang, K.-P., Sim, J. H., Khoo, C. H., Fairuz, Z. A., Halim, S. N. B. A., Ng, S. W., Seng, H.-L. & Tiekink, E. R. T. (2013). *Eur. J. Med. Chem.* **67**, 127–141.
- Khan, N., Farina, Y., Mun, L. K., Rajab, N. F. & Awang, N. (2015). *Polyhedron*, **85**, 754–760.
- Li, H., Lai, C. S., Wu, J., Ho, P. C., de Vos, D. & Tiekink, E. R. T. (2007). *J. Inorg. Biochem.* **101**, 809–816.
- Lindley, P. F. & Carr, P. (1974). *J. Cryst. Mol. Struct.* **4**, 173–185.
- Mohamad, R., Awang, N., Jotani, M. M. & Tiekink, E. R. T. (2016). *Acta Cryst.* **E72**, 1130–1137.
- Mohamad, R., Awang, N., Kamaludin, N. F. & Abu Bakar, N. F. (2016). *Res. J. Pharm. Biol. Chem. Sci.* **7**, 1269–1274.
- Mohamad, R., Awang, N., Kamaludin, N. F., Jotani, M. M. & Tiekink, E. R. T. (2017). *Acta Cryst.* **E73**, 260–265.
- Mohamad, R., Awang, N., Kamaludin, N. F., Jotani, M. M. & Tiekink, E. R. T. (2018a). *Acta Cryst.* **E74**, 302–308.
- Mohamad, R., Awang, N., Kamaludin, N. F., Jotani, M. M. & Tiekink, E. R. T. (2018b). *Acta Cryst.* **E74**, 630–637.
- Ramasamy, K., Kuznetsov, V. L., Gopal, K., Malik, M. A., Raftery, J., Edwards, P. P. & O'Brien, P. (2013). *Chem. Mater.* **25**, 266–276.
- Rigaku OD (2018). *CrysAlis PRO* Software system. Rigaku Corporation, Oxford, UK.
- Sheldrick, G. M. (2015a). *Acta Cryst.* **A71**, 3–8.
- Sheldrick, G. M. (2015b). *Acta Cryst.* **C71**, 3–8.
- Sim, J.-H., Jamaludin, N. S., Khoo, C.-H., Cheah, Y.-K., Halim, S. N. B. A., Seng, H.-L. & Tiekink, E. R. T. (2014). *Gold Bull.* **47**, 225–236.
- Spek, A. L. (2020). *Acta Cryst.* **E76**, 1–11.
- Tan, S. L., Jotani, M. M. & Tiekink, E. R. T. (2019). *Acta Cryst.* **E75**, 308–318.
- Tan, Y. J., Tan, Y. S., Yeo, C. I., Chew, J. & Tiekink, E. R. T. (2019). *J. Inorg. Biochem.* **192**, 107–118.
- Tan, Y. S., Ooi, K. K., Ang, K. P., Akim, A. M., Cheah, Y.-K., Halim, S. N. A., Seng, H.-L. & Tiekink, E. R. T. (2015). *J. Inorg. Biochem.* **150**, 48–62.
- Tiekink, E. R. T. (2008). *Appl. Organomet. Chem.* **22**, 533–550.
- Turner, M. J., Mckinnon, J. J., Wolff, S. K., Grimwood, D. J., Spackman, P. R., Jayatilaka, D. & Spackman, M. A. (2017). *Crystal Explorer v17*. The University of Western Australia.
- Westrip, S. P. (2010). *J. Appl. Cryst.* **43**, 920–925.

supporting information

Acta Cryst. (2020). E76, 167-176 [https://doi.org/10.1107/S2056989020000122]

(*N,N*-Diallyldithiocarbamato- κ^2 S,S')triphenyltin(IV) and bis(*N,N*-diallyldithiocarbamato- κ^2 S,S')diphenyltin(IV): crystal structure, Hirshfeld surface analysis and computational study

Farah Natasha Haezam, Normah Awang, Nurul Farahana Kamaludin, Mukesh M. Jotani and Edward R. T. Tiekink

Computing details

For both structures, data collection: *CrysAlis PRO* (Rigaku OD, 2018); cell refinement: *CrysAlis PRO* (Rigaku OD, 2018); data reduction: *CrysAlis PRO* (Rigaku OD, 2018); program(s) used to solve structure: *SHELXS* (Sheldrick, 2015a); program(s) used to refine structure: *SHELXL2017/1* (Sheldrick, 2015b); molecular graphics: *ORTEP-3 for Windows* (Farrugia, 2012), *DIAMOND* (Brandenburg, 2006); software used to prepare material for publication: *publCIF* (Westrip, 2010).

(*N,N*-Diallyldithiocarbamato- κ^2 S,S')\ triphenyltin(IV) (I)

Crystal data

[Sn(C₆H₅)₃(C₇H₁₀NS₂)]

$M_r = 522.27$

Monoclinic, *P2₁/c*

$a = 8.0650$ (1) Å

$b = 11.4490$ (1) Å

$c = 25.8775$ (2) Å

$\beta = 98.282$ (1)°

$V = 2364.51$ (4) Å³

$Z = 4$

$F(000) = 1056$

$D_x = 1.467$ Mg m⁻³

Cu $K\alpha$ radiation, $\lambda = 1.54184$ Å

Cell parameters from 34049 reflections

$\theta = 3.4\text{--}76.3^\circ$

$\mu = 10.32$ mm⁻¹

$T = 100$ K

Prism, colourless

$0.13 \times 0.10 \times 0.04$ mm

Data collection

XtaLAB Synergy, Dualflex, AtlasS2
diffractometer

Radiation source: micro-focus sealed X-ray
tube, PhotonJet (Cu) X-ray Source

Mirror monochromator

Detector resolution: 5.2558 pixels mm⁻¹

ω scans

Absorption correction: gaussian
(*CrysAlis PRO*; Rigaku OD, 2018)

$T_{\min} = 0.807$, $T_{\max} = 1.000$

55086 measured reflections

4226 independent reflections

4083 reflections with $I > 2\sigma(I)$

$R_{\text{int}} = 0.044$

$\theta_{\max} = 67.1^\circ$, $\theta_{\min} = 3.5^\circ$

$h = -9 \rightarrow 9$

$k = -13 \rightarrow 13$

$l = -26 \rightarrow 30$

Refinement

Refinement on F^2

Least-squares matrix: full

$R[F^2 > 2\sigma(F^2)] = 0.020$

$wR(F^2) = 0.053$

$S = 1.01$

4226 reflections

262 parameters

0 restraints

Primary atom site location: structure-invariant
direct methods

Secondary atom site location: difference Fourier
map

Hydrogen site location: inferred from
neighbouring sites

H-atom parameters constrained

$w = 1/[\sigma^2(F_o^2) + (0.034P)^2 + 1.0941P]$

where $P = (F_o^2 + 2F_c^2)/3$

$(\Delta/\sigma)_{\max} = 0.001$

$\Delta\rho_{\max} = 0.82 \text{ e } \text{\AA}^{-3}$

$\Delta\rho_{\min} = -0.50 \text{ e } \text{\AA}^{-3}$

Special details

Geometry. All esds (except the esd in the dihedral angle between two l.s. planes) are estimated using the full covariance matrix. The cell esds are taken into account individually in the estimation of esds in distances, angles and torsion angles; correlations between esds in cell parameters are only used when they are defined by crystal symmetry. An approximate (isotropic) treatment of cell esds is used for estimating esds involving l.s. planes.

Fractional atomic coordinates and isotropic or equivalent isotropic displacement parameters (\AA^2)

	x	y	z	$U_{\text{iso}}^*/U_{\text{eq}}$
Sn	0.25851 (2)	0.27508 (2)	0.37027 (2)	0.01943 (6)
S1	0.40753 (6)	0.34500 (4)	0.45492 (2)	0.02546 (11)
S2	0.50865 (6)	0.11062 (4)	0.42287 (2)	0.02585 (11)
N1	0.6650 (2)	0.22704 (13)	0.50510 (7)	0.0221 (3)
C1	0.5424 (2)	0.22413 (16)	0.46477 (8)	0.0211 (4)
C2	0.6883 (2)	0.32426 (18)	0.54246 (8)	0.0267 (4)
H2A	0.646687	0.397215	0.524565	0.032*
H2B	0.809419	0.334224	0.554922	0.032*
C3	0.5978 (3)	0.3042 (2)	0.58847 (8)	0.0309 (5)
H3	0.612847	0.360684	0.615638	0.037*
C4	0.4992 (3)	0.2149 (2)	0.59435 (9)	0.0319 (5)
H4A	0.480682	0.156449	0.568121	0.038*
H4B	0.446654	0.209057	0.624828	0.038*
C5	0.7846 (2)	0.12945 (18)	0.51605 (8)	0.0249 (4)
H5A	0.732148	0.056406	0.501157	0.030*
H5B	0.812801	0.118925	0.554284	0.030*
C6	0.9410 (3)	0.1527 (2)	0.49311 (9)	0.0315 (4)
H6	0.931935	0.161093	0.456289	0.038*
C7	1.0904 (3)	0.1621 (2)	0.52078 (11)	0.0427 (6)
H7A	1.103510	0.154114	0.557684	0.051*
H7B	1.185305	0.176968	0.503870	0.051*
C11	0.0883 (2)	0.13134 (16)	0.35523 (7)	0.0204 (4)
C12	-0.0823 (2)	0.15586 (18)	0.34399 (7)	0.0257 (4)
H12	-0.120299	0.233677	0.347295	0.031*
C13	-0.1979 (2)	0.06837 (19)	0.32802 (8)	0.0278 (4)
H13	-0.313765	0.086573	0.320597	0.033*
C14	-0.1442 (3)	-0.04484 (19)	0.32295 (8)	0.0279 (4)
H14	-0.222732	-0.104752	0.311737	0.033*

C15	0.0259 (3)	-0.07077 (18)	0.33438 (9)	0.0308 (4)
H15	0.063245	-0.148801	0.331218	0.037*
C16	0.1410 (2)	0.01651 (17)	0.35033 (8)	0.0254 (4)
H16	0.256747	-0.002093	0.357990	0.030*
C21	0.4161 (2)	0.28918 (16)	0.31120 (7)	0.0213 (4)
C22	0.5403 (2)	0.37446 (18)	0.31258 (8)	0.0269 (4)
H22	0.554696	0.429581	0.340305	0.032*
C23	0.6428 (3)	0.37983 (19)	0.27407 (9)	0.0312 (5)
H23	0.726432	0.438594	0.275407	0.037*
C24	0.6234 (3)	0.2996 (2)	0.23361 (9)	0.0313 (5)
H24	0.693634	0.303209	0.207178	0.038*
C25	0.5010 (3)	0.21372 (18)	0.23174 (8)	0.0280 (4)
H25	0.487954	0.158250	0.204148	0.034*
C26	0.3979 (2)	0.20907 (17)	0.27018 (8)	0.0223 (4)
H26	0.313726	0.150577	0.268562	0.027*
C31	0.0978 (2)	0.42764 (17)	0.36369 (8)	0.0242 (4)
C32	-0.0065 (3)	0.45310 (18)	0.40077 (8)	0.0293 (4)
H32	-0.007314	0.402694	0.429894	0.035*
C33	-0.1095 (3)	0.5512 (2)	0.39575 (10)	0.0357 (5)
H33	-0.180213	0.567475	0.421210	0.043*
C34	-0.1081 (3)	0.62513 (19)	0.35328 (10)	0.0374 (5)
H34	-0.177793	0.692406	0.349818	0.045*
C35	-0.0067 (3)	0.60157 (19)	0.31626 (9)	0.0350 (5)
H35	-0.006485	0.652566	0.287313	0.042*
C36	0.0959 (2)	0.50318 (18)	0.32102 (8)	0.0273 (4)
H36	0.165193	0.487164	0.295126	0.033*

Atomic displacement parameters (\AA^2)

	U^{11}	U^{22}	U^{33}	U^{12}	U^{13}	U^{23}
Sn	0.02063 (8)	0.01640 (8)	0.02001 (8)	0.00251 (4)	-0.00135 (5)	-0.00007 (4)
S1	0.0271 (2)	0.0215 (2)	0.0253 (2)	0.00683 (18)	-0.00475 (18)	-0.00472 (17)
S2	0.0301 (2)	0.0205 (2)	0.0254 (2)	0.00408 (18)	-0.00133 (18)	-0.00396 (18)
N1	0.0206 (8)	0.0200 (9)	0.0246 (8)	0.0016 (6)	-0.0007 (7)	0.0000 (6)
C1	0.0186 (9)	0.0212 (10)	0.0232 (9)	0.0002 (7)	0.0025 (7)	0.0024 (7)
C2	0.0249 (10)	0.0223 (10)	0.0303 (10)	-0.0022 (8)	-0.0051 (8)	-0.0028 (8)
C3	0.0314 (11)	0.0333 (11)	0.0255 (10)	0.0014 (9)	-0.0043 (8)	-0.0109 (9)
C4	0.0289 (11)	0.0404 (13)	0.0257 (10)	0.0021 (9)	0.0015 (8)	-0.0050 (8)
C5	0.0215 (9)	0.0240 (10)	0.0282 (10)	0.0029 (8)	0.0005 (7)	0.0037 (8)
C6	0.0285 (10)	0.0312 (11)	0.0356 (11)	0.0057 (9)	0.0074 (9)	0.0036 (9)
C7	0.0255 (11)	0.0398 (14)	0.0632 (16)	0.0002 (10)	0.0083 (10)	0.0010 (12)
C11	0.0245 (9)	0.0192 (9)	0.0173 (8)	0.0018 (7)	0.0029 (7)	0.0011 (7)
C12	0.0245 (9)	0.0241 (10)	0.0270 (9)	0.0061 (8)	-0.0013 (8)	-0.0026 (8)
C13	0.0212 (9)	0.0328 (11)	0.0279 (10)	0.0015 (8)	-0.0011 (7)	0.0008 (8)
C14	0.0278 (10)	0.0268 (11)	0.0296 (10)	-0.0080 (8)	0.0059 (8)	-0.0019 (8)
C15	0.0298 (10)	0.0187 (10)	0.0453 (12)	-0.0004 (8)	0.0107 (9)	-0.0025 (9)
C16	0.0233 (9)	0.0190 (10)	0.0347 (10)	0.0017 (8)	0.0069 (8)	-0.0005 (8)
C21	0.0203 (9)	0.0204 (9)	0.0215 (9)	0.0019 (7)	-0.0024 (7)	0.0036 (7)

C22	0.0260 (10)	0.0203 (10)	0.0320 (10)	-0.0032 (8)	-0.0037 (8)	0.0013 (8)
C23	0.0235 (10)	0.0288 (11)	0.0396 (11)	-0.0078 (8)	-0.0012 (8)	0.0090 (9)
C24	0.0230 (10)	0.0387 (12)	0.0325 (11)	-0.0006 (9)	0.0051 (8)	0.0097 (9)
C25	0.0276 (10)	0.0297 (11)	0.0258 (10)	-0.0019 (8)	0.0006 (8)	0.0010 (8)
C26	0.0206 (9)	0.0224 (9)	0.0227 (9)	-0.0032 (7)	-0.0004 (7)	0.0022 (7)
C31	0.0226 (9)	0.0154 (9)	0.0318 (10)	0.0013 (7)	-0.0053 (8)	-0.0033 (7)
C32	0.0284 (10)	0.0207 (10)	0.0366 (11)	0.0016 (8)	-0.0022 (8)	-0.0044 (8)
C33	0.0245 (10)	0.0270 (11)	0.0534 (13)	0.0010 (9)	-0.0018 (9)	-0.0144 (10)
C34	0.0263 (10)	0.0179 (10)	0.0621 (15)	0.0029 (8)	-0.0139 (10)	-0.0059 (10)
C35	0.0306 (11)	0.0205 (10)	0.0481 (13)	-0.0019 (9)	-0.0140 (10)	0.0033 (9)
C36	0.0247 (9)	0.0201 (10)	0.0331 (10)	-0.0016 (8)	-0.0099 (8)	-0.0001 (8)

Geometric parameters (Å, °)

Sn—C21	2.130 (2)	C13—H13	0.9500
Sn—C11	2.1427 (19)	C14—C15	1.393 (3)
Sn—C31	2.1673 (19)	C14—H14	0.9500
Sn—S1	2.4749 (4)	C15—C16	1.386 (3)
Sn—S2	2.9456 (5)	C15—H15	0.9500
S1—C1	1.7559 (19)	C16—H16	0.9500
S2—C1	1.6894 (19)	C21—C26	1.394 (3)
N1—C1	1.330 (3)	C21—C22	1.395 (3)
N1—C2	1.468 (3)	C22—C23	1.384 (3)
N1—C5	1.477 (2)	C22—H22	0.9500
C2—C3	1.502 (3)	C23—C24	1.385 (3)
C2—H2A	0.9900	C23—H23	0.9500
C2—H2B	0.9900	C24—C25	1.388 (3)
C3—C4	1.317 (3)	C24—H24	0.9500
C3—H3	0.9500	C25—C26	1.387 (3)
C4—H4A	0.9500	C25—H25	0.9500
C4—H4B	0.9500	C26—H26	0.9500
C5—C6	1.493 (3)	C31—C32	1.395 (3)
C5—H5A	0.9900	C31—C36	1.401 (3)
C5—H5B	0.9900	C32—C33	1.392 (3)
C6—C7	1.315 (3)	C32—H32	0.9500
C6—H6	0.9500	C33—C34	1.388 (4)
C7—H7A	0.9500	C33—H33	0.9500
C7—H7B	0.9500	C34—C35	1.373 (4)
C11—C12	1.393 (3)	C34—H34	0.9500
C11—C16	1.393 (3)	C35—C36	1.393 (3)
C12—C13	1.390 (3)	C35—H35	0.9500
C12—H12	0.9500	C36—H36	0.9500
C13—C14	1.379 (3)		
C21—Sn—C11	111.15 (7)	C14—C13—C12	119.99 (18)
C21—Sn—C31	107.13 (7)	C14—C13—H13	120.0
C11—Sn—C31	104.14 (7)	C12—C13—H13	120.0
C21—Sn—S1	110.28 (5)	C13—C14—C15	119.53 (19)

C11—Sn—S1	128.76 (5)	C13—C14—H14	120.2
C31—Sn—S1	91.01 (5)	C15—C14—H14	120.2
C21—Sn—S2	86.57 (5)	C16—C15—C14	120.43 (19)
C11—Sn—S2	88.36 (5)	C16—C15—H15	119.8
C31—Sn—S2	156.01 (5)	C14—C15—H15	119.8
S1—Sn—S2	65.470 (14)	C15—C16—C11	120.48 (18)
C1—S1—Sn	94.89 (7)	C15—C16—H16	119.8
C1—S2—Sn	80.86 (6)	C11—C16—H16	119.8
C1—N1—C2	123.08 (16)	C26—C21—C22	118.46 (19)
C1—N1—C5	121.51 (16)	C26—C21—Sn	119.19 (14)
C2—N1—C5	115.39 (15)	C22—C21—Sn	122.33 (15)
N1—C1—S2	123.75 (14)	C23—C22—C21	120.87 (19)
N1—C1—S1	117.96 (14)	C23—C22—H22	119.6
S2—C1—S1	118.29 (11)	C21—C22—H22	119.6
N1—C2—C3	112.04 (17)	C22—C23—C24	120.03 (19)
N1—C2—H2A	109.2	C22—C23—H23	120.0
C3—C2—H2A	109.2	C24—C23—H23	120.0
N1—C2—H2B	109.2	C23—C24—C25	119.9 (2)
C3—C2—H2B	109.2	C23—C24—H24	120.1
H2A—C2—H2B	107.9	C25—C24—H24	120.1
C4—C3—C2	125.52 (19)	C26—C25—C24	119.9 (2)
C4—C3—H3	117.2	C26—C25—H25	120.0
C2—C3—H3	117.2	C24—C25—H25	120.0
C3—C4—H4A	120.0	C25—C26—C21	120.81 (18)
C3—C4—H4B	120.0	C25—C26—H26	119.6
H4A—C4—H4B	120.0	C21—C26—H26	119.6
N1—C5—C6	110.80 (17)	C32—C31—C36	118.31 (19)
N1—C5—H5A	109.5	C32—C31—Sn	121.84 (15)
C6—C5—H5A	109.5	C36—C31—Sn	119.85 (15)
N1—C5—H5B	109.5	C31—C32—C33	121.0 (2)
C6—C5—H5B	109.5	C31—C32—H32	119.5
H5A—C5—H5B	108.1	C33—C32—H32	119.5
C7—C6—C5	124.0 (2)	C34—C33—C32	119.6 (2)
C7—C6—H6	118.0	C34—C33—H33	120.2
C5—C6—H6	118.0	C32—C33—H33	120.2
C6—C7—H7A	120.0	C35—C34—C33	120.4 (2)
C6—C7—H7B	120.0	C35—C34—H34	119.8
H7A—C7—H7B	120.0	C33—C34—H34	119.8
C12—C11—C16	118.46 (18)	C34—C35—C36	120.2 (2)
C12—C11—Sn	118.09 (14)	C34—C35—H35	119.9
C16—C11—Sn	123.03 (14)	C36—C35—H35	119.9
C13—C12—C11	121.09 (19)	C35—C36—C31	120.5 (2)
C13—C12—H12	119.5	C35—C36—H36	119.7
C11—C12—H12	119.5	C31—C36—H36	119.7
C2—N1—C1—S2	-177.36 (15)	C14—C15—C16—C11	0.1 (3)
C5—N1—C1—S2	0.8 (3)	C12—C11—C16—C15	0.3 (3)
C2—N1—C1—S1	2.3 (3)	Sn—C11—C16—C15	-172.13 (15)

C5—N1—C1—S1	-179.62 (14)	C26—C21—C22—C23	0.2 (3)
Sn—S2—C1—N1	-174.18 (18)	Sn—C21—C22—C23	178.75 (15)
Sn—S2—C1—S1	6.21 (10)	C21—C22—C23—C24	-0.3 (3)
Sn—S1—C1—N1	173.04 (15)	C22—C23—C24—C25	0.0 (3)
Sn—S1—C1—S2	-7.33 (12)	C23—C24—C25—C26	0.4 (3)
C1—N1—C2—C3	91.6 (2)	C24—C25—C26—C21	-0.5 (3)
C5—N1—C2—C3	-86.6 (2)	C22—C21—C26—C25	0.2 (3)
N1—C2—C3—C4	-4.2 (3)	Sn—C21—C26—C25	-178.38 (15)
C1—N1—C5—C6	95.9 (2)	C36—C31—C32—C33	-0.3 (3)
C2—N1—C5—C6	-85.9 (2)	Sn—C31—C32—C33	-179.70 (14)
N1—C5—C6—C7	118.2 (2)	C31—C32—C33—C34	-0.2 (3)
C16—C11—C12—C13	-0.3 (3)	C32—C33—C34—C35	0.3 (3)
Sn—C11—C12—C13	172.55 (15)	C33—C34—C35—C36	0.0 (3)
C11—C12—C13—C14	-0.2 (3)	C34—C35—C36—C31	-0.4 (3)
C12—C13—C14—C15	0.6 (3)	C32—C31—C36—C35	0.6 (3)
C13—C14—C15—C16	-0.5 (3)	Sn—C31—C36—C35	-179.98 (14)

Hydrogen-bond geometry (\AA , $^\circ$)

$Cg1$ and $Cg2$ are the centroids of the (C21–C26) and (C31–C36) rings, respectively.

$D—H\cdots A$	$D—H$	$H\cdots A$	$D\cdots A$	$D—H\cdots A$
C13—H13 $\cdots Cg1^i$	0.95	2.92	3.605 (2)	130
C23—H23 $\cdots Cg2^{ii}$	0.95	2.99	3.720 (3)	134

Symmetry codes: (i) $x-1, y, z$; (ii) $x+1, y, z$.

Bis(*N,N*-diallyldithiocarbamato- κ^2S,S')diphenyltin(IV) (II)*Crystal data*

$[\text{Sn}(\text{C}_6\text{H}_5)_2(\text{C}_7\text{H}_{10}\text{NS}_2)_2]$

$M_r = 617.45$

Monoclinic, $P2_1/c$

$a = 9.6160$ (1) \AA

$b = 30.4216$ (2) \AA

$c = 19.1928$ (1) \AA

$\beta = 100.019$ (1) $^\circ$

$V = 5528.93$ (8) \AA^3

$Z = 8$

$F(000) = 2512$

$D_x = 1.484$ Mg m^{-3}

Cu $K\alpha$ radiation, $\lambda = 1.54184$ \AA

Cell parameters from 40535 reflections

$\theta = 2.9\text{--}76.3^\circ$

$\mu = 10.30$ mm^{-1}

$T = 100$ K

Prism, colourless

$0.19 \times 0.14 \times 0.07$ mm

Data collection

XtaLAB Synergy, Dualflex, AtlasS2
diffractometer

Radiation source: micro-focus sealed X-ray
tube, PhotonJet (Cu) X-ray Source

Mirror monochromator

Detector resolution: 5.2558 pixels mm^{-1}

ω scans

Absorption correction: gaussian
(CrysAlisPro; Rigaku OD, 2018)

$T_{\min} = 0.633$, $T_{\max} = 1.000$

67735 measured reflections

9876 independent reflections

9370 reflections with $I > 2\sigma(I)$

$R_{\text{int}} = 0.037$

$\theta_{\max} = 67.1^\circ$, $\theta_{\min} = 3.7^\circ$

$h = -11 \rightarrow 11$

$k = -36 \rightarrow 25$

$l = -22 \rightarrow 22$

Refinement

Refinement on F^2
 Least-squares matrix: full
 $R[F^2 > 2\sigma(F^2)] = 0.027$
 $wR(F^2) = 0.068$
 $S = 1.01$
 9876 reflections
 595 parameters
 0 restraints
 Primary atom site location: structure-invariant
 direct methods

Secondary atom site location: difference Fourier
 map
 Hydrogen site location: inferred from
 neighbouring sites
 H-atom parameters constrained
 $w = 1/[\sigma^2(F_o^2) + (0.0362P)^2 + 7.0312P]$
 where $P = (F_o^2 + 2F_c^2)/3$
 $(\Delta/\sigma)_{\max} = 0.003$
 $\Delta\rho_{\max} = 1.23 \text{ e } \text{\AA}^{-3}$
 $\Delta\rho_{\min} = -0.73 \text{ e } \text{\AA}^{-3}$

Special details

Geometry. All esds (except the esd in the dihedral angle between two l.s. planes) are estimated using the full covariance matrix. The cell esds are taken into account individually in the estimation of esds in distances, angles and torsion angles; correlations between esds in cell parameters are only used when they are defined by crystal symmetry. An approximate (isotropic) treatment of cell esds is used for estimating esds involving l.s. planes.

Fractional atomic coordinates and isotropic or equivalent isotropic displacement parameters (\AA^2)

	<i>x</i>	<i>y</i>	<i>z</i>	$U_{\text{iso}}^*/U_{\text{eq}}$
Sn1	0.96840 (2)	0.26758 (2)	0.60783 (2)	0.01863 (5)
S1	1.05093 (7)	0.34237 (2)	0.65910 (3)	0.02202 (13)
S2	1.05034 (7)	0.32188 (2)	0.50854 (3)	0.02481 (13)
S3	0.82312 (7)	0.21606 (2)	0.51668 (4)	0.02761 (14)
S4	0.71629 (7)	0.30174 (2)	0.55382 (3)	0.02345 (13)
N1	1.1264 (2)	0.39971 (7)	0.56894 (11)	0.0203 (4)
N2	0.5656 (2)	0.24617 (7)	0.46333 (12)	0.0253 (5)
C1	1.0824 (2)	0.35895 (8)	0.57638 (13)	0.0189 (5)
C2	1.1517 (3)	0.41701 (9)	0.50102 (14)	0.0251 (6)
H2A	1.121986	0.448186	0.496767	0.030*
H2B	1.093159	0.400473	0.462164	0.030*
C3	1.3039 (3)	0.41377 (9)	0.49308 (14)	0.0286 (6)
H3	1.331520	0.429629	0.455081	0.034*
C4	1.4027 (3)	0.39104 (10)	0.53379 (16)	0.0309 (6)
H4A	1.380189	0.374657	0.572463	0.037*
H4B	1.496585	0.391033	0.524485	0.037*
C5	1.1518 (3)	0.43140 (8)	0.62834 (14)	0.0225 (5)
H5A	1.229774	0.451427	0.621918	0.027*
H5B	1.180874	0.415255	0.673303	0.027*
C6	1.0221 (3)	0.45784 (9)	0.63244 (13)	0.0246 (5)
H6	0.938442	0.442486	0.637625	0.030*
C7	1.0169 (3)	0.50095 (10)	0.62931 (15)	0.0312 (6)
H7A	1.098766	0.517238	0.624141	0.037*
H7B	0.931250	0.515847	0.632218	0.037*
C8	0.6860 (3)	0.25402 (8)	0.50603 (13)	0.0211 (5)
C9	0.4473 (3)	0.27826 (9)	0.45194 (15)	0.0270 (6)
H9A	0.459611	0.299926	0.491021	0.032*
H9B	0.356671	0.262729	0.451561	0.032*

C10	0.4444 (3)	0.30145 (11)	0.38295 (16)	0.0357 (7)
H10	0.513805	0.323315	0.380204	0.043*
C11	0.3516 (4)	0.29318 (13)	0.32636 (18)	0.0485 (9)
H11A	0.281054	0.271475	0.327679	0.058*
H11B	0.354463	0.308876	0.283842	0.058*
C12	0.5396 (3)	0.20533 (10)	0.42143 (16)	0.0341 (7)
H12A	0.630727	0.190610	0.419544	0.041*
H12B	0.494638	0.212628	0.372403	0.041*
C13	0.4460 (4)	0.17484 (10)	0.45334 (18)	0.0415 (8)
H13	0.483016	0.161495	0.497427	0.050*
C14	0.3162 (4)	0.16547 (13)	0.4240 (3)	0.0601 (11)
H14A	0.276367	0.178312	0.379956	0.072*
H14B	0.261771	0.145828	0.446853	0.072*
C15	1.1604 (3)	0.22965 (8)	0.61670 (13)	0.0210 (5)
C16	1.2902 (3)	0.24774 (9)	0.60881 (14)	0.0247 (5)
H16	1.295812	0.277867	0.596567	0.030*
C17	1.4111 (3)	0.22188 (9)	0.61878 (16)	0.0289 (6)
H17	1.499314	0.234539	0.614001	0.035*
C18	1.4039 (3)	0.17786 (9)	0.63562 (14)	0.0273 (6)
H18	1.486760	0.160247	0.641839	0.033*
C19	1.2754 (3)	0.15942 (9)	0.64342 (14)	0.0256 (6)
H19	1.270001	0.129177	0.654966	0.031*
C20	1.1552 (3)	0.18534 (9)	0.63427 (13)	0.0230 (5)
H20	1.067687	0.172668	0.640090	0.028*
C21	0.8975 (3)	0.24718 (8)	0.70441 (13)	0.0203 (5)
C22	0.9742 (3)	0.26067 (9)	0.76923 (14)	0.0265 (6)
H22	1.055704	0.278445	0.770037	0.032*
C23	0.9342 (3)	0.24871 (10)	0.83264 (15)	0.0323 (6)
H23	0.988359	0.258258	0.876175	0.039*
C24	0.8158 (3)	0.22295 (10)	0.83270 (16)	0.0317 (6)
H24	0.787943	0.214921	0.876082	0.038*
C25	0.7383 (3)	0.20897 (10)	0.76898 (16)	0.0327 (6)
H25	0.656701	0.191282	0.768520	0.039*
C26	0.7797 (3)	0.22080 (9)	0.70546 (15)	0.0266 (6)
H26	0.726533	0.210653	0.662062	0.032*
Sn2	0.42934 (2)	0.47935 (2)	0.26224 (2)	0.01967 (5)
S1A	0.50653 (7)	0.43729 (2)	0.15999 (3)	0.02630 (14)
S2A	0.65505 (7)	0.51843 (2)	0.21454 (3)	0.02630 (14)
S3A	0.39019 (7)	0.55322 (2)	0.32085 (3)	0.02589 (14)
S4A	0.29651 (7)	0.53675 (2)	0.16787 (3)	0.02586 (14)
N1A	0.6984 (2)	0.47703 (7)	0.09775 (12)	0.0264 (5)
N2A	0.2774 (2)	0.61450 (7)	0.22935 (11)	0.0229 (4)
C1A	0.6292 (3)	0.47819 (8)	0.15187 (14)	0.0234 (5)
C2A	0.6696 (3)	0.44435 (10)	0.03990 (15)	0.0328 (6)
H2A1	0.675651	0.458786	−0.005706	0.039*
H2A2	0.572710	0.432678	0.037076	0.039*
C3A	0.7733 (4)	0.40729 (10)	0.05215 (16)	0.0375 (7)
H3A	0.763123	0.386079	0.087245	0.045*

C4A	0.8781 (4)	0.40263 (11)	0.01660 (17)	0.0400 (7)
H4A1	0.890527	0.423401	−0.018758	0.048*
H4A2	0.941186	0.378490	0.026373	0.048*
C5A	0.8112 (3)	0.50881 (10)	0.09071 (15)	0.0280 (6)
H5A1	0.888230	0.493556	0.072253	0.034*
H5A2	0.850815	0.520988	0.137826	0.034*
C6A	0.7561 (4)	0.54519 (12)	0.04217 (19)	0.0446 (8)
H6A	0.688042	0.564544	0.055802	0.053*
C7A	0.7971 (5)	0.55184 (17)	−0.0189 (2)	0.0720 (15)
H7A1	0.865062	0.532902	−0.033670	0.086*
H7A2	0.758874	0.575581	−0.048313	0.086*
C8A	0.3158 (3)	0.57268 (8)	0.23782 (13)	0.0221 (5)
C9A	0.2113 (3)	0.63244 (9)	0.16070 (14)	0.0254 (6)
H9A1	0.250124	0.617093	0.122830	0.030*
H9A2	0.236138	0.663945	0.158775	0.030*
C10A	0.0529 (3)	0.62794 (9)	0.14665 (14)	0.0270 (6)
H10A	0.003035	0.643092	0.106705	0.032*
C11A	−0.0226 (3)	0.60500 (9)	0.18449 (15)	0.0296 (6)
H11C	0.022624	0.589294	0.224927	0.036*
H11D	−0.122521	0.604126	0.171420	0.036*
C12A	0.3060 (3)	0.64644 (9)	0.28729 (15)	0.0262 (6)
H12C	0.306030	0.631114	0.332786	0.031*
H12D	0.229511	0.668611	0.281445	0.031*
C13A	0.4451 (3)	0.66935 (9)	0.28974 (15)	0.0304 (6)
H13A	0.461271	0.694727	0.318873	0.036*
C14A	0.5464 (3)	0.65786 (11)	0.25573 (16)	0.0345 (7)
H14C	0.535363	0.632722	0.225908	0.041*
H14D	0.630812	0.674669	0.260903	0.041*
C15A	0.5755 (3)	0.45369 (8)	0.35224 (13)	0.0199 (5)
C16A	0.6517 (3)	0.41536 (9)	0.34627 (15)	0.0262 (6)
H16A	0.641902	0.400827	0.301871	0.031*
C17A	0.7420 (3)	0.39798 (9)	0.40436 (16)	0.0281 (6)
H17A	0.792462	0.371612	0.399584	0.034*
C18A	0.7580 (3)	0.41916 (9)	0.46894 (15)	0.0267 (6)
H18A	0.819483	0.407280	0.508595	0.032*
C19A	0.6849 (3)	0.45768 (9)	0.47610 (14)	0.0263 (6)
H19A	0.696848	0.472399	0.520395	0.032*
C20A	0.5935 (3)	0.47474 (9)	0.41787 (14)	0.0222 (5)
H20A	0.542863	0.501025	0.422959	0.027*
C21A	0.2380 (3)	0.44192 (9)	0.26420 (13)	0.0219 (5)
C22A	0.2467 (3)	0.40539 (9)	0.30792 (14)	0.0263 (6)
H22A	0.335183	0.397555	0.335339	0.032*
C23A	0.1275 (3)	0.37983 (10)	0.31248 (16)	0.0322 (6)
H23A	0.135091	0.355207	0.343351	0.039*
C24A	−0.0010 (3)	0.39055 (10)	0.27192 (16)	0.0330 (6)
H24A	−0.082123	0.373216	0.274518	0.040*
C25A	−0.0111 (3)	0.42636 (11)	0.22781 (17)	0.0387 (7)
H25A	−0.099646	0.433692	0.199882	0.046*

C26A	0.1072 (3)	0.45212 (10)	0.22356 (16)	0.0333 (6)
H26A	0.098571	0.476793	0.192762	0.040*

Atomic displacement parameters (Å²)

	U^{11}	U^{22}	U^{33}	U^{12}	U^{13}	U^{23}
Sn1	0.01673 (9)	0.01771 (9)	0.02066 (9)	0.00008 (6)	0.00108 (6)	0.00380 (6)
S1	0.0246 (3)	0.0185 (3)	0.0228 (3)	-0.0030 (2)	0.0037 (2)	0.0032 (2)
S2	0.0267 (3)	0.0227 (3)	0.0238 (3)	0.0006 (2)	0.0011 (2)	-0.0032 (2)
S3	0.0280 (3)	0.0230 (3)	0.0299 (3)	0.0049 (3)	-0.0003 (3)	-0.0037 (3)
S4	0.0229 (3)	0.0177 (3)	0.0279 (3)	-0.0001 (2)	-0.0008 (2)	0.0003 (2)
N1	0.0208 (10)	0.0202 (10)	0.0198 (10)	-0.0006 (8)	0.0031 (8)	0.0034 (8)
N2	0.0270 (12)	0.0218 (11)	0.0267 (11)	0.0017 (9)	0.0031 (9)	-0.0053 (9)
C1	0.0168 (11)	0.0178 (12)	0.0212 (12)	0.0021 (9)	0.0004 (9)	0.0021 (10)
C2	0.0292 (14)	0.0255 (13)	0.0203 (13)	-0.0022 (11)	0.0035 (11)	0.0061 (10)
C3	0.0339 (15)	0.0307 (15)	0.0231 (13)	-0.0093 (12)	0.0099 (11)	-0.0019 (11)
C4	0.0255 (14)	0.0323 (15)	0.0362 (15)	-0.0045 (12)	0.0093 (12)	-0.0052 (12)
C5	0.0251 (13)	0.0183 (12)	0.0236 (13)	-0.0054 (10)	0.0026 (10)	-0.0003 (10)
C6	0.0282 (14)	0.0231 (13)	0.0218 (13)	-0.0027 (11)	0.0026 (10)	-0.0005 (10)
C7	0.0343 (15)	0.0277 (15)	0.0315 (15)	0.0037 (12)	0.0056 (12)	0.0024 (12)
C8	0.0230 (13)	0.0207 (12)	0.0198 (12)	0.0003 (10)	0.0046 (10)	0.0007 (10)
C9	0.0195 (13)	0.0303 (14)	0.0299 (14)	0.0020 (11)	0.0010 (11)	-0.0008 (12)
C10	0.0301 (15)	0.0400 (17)	0.0379 (17)	0.0053 (13)	0.0085 (13)	0.0092 (13)
C11	0.052 (2)	0.057 (2)	0.0348 (17)	0.0146 (18)	0.0035 (15)	0.0080 (16)
C12	0.0331 (15)	0.0317 (15)	0.0350 (16)	-0.0014 (13)	-0.0007 (12)	-0.0153 (13)
C13	0.057 (2)	0.0245 (15)	0.0402 (17)	-0.0038 (14)	0.0013 (15)	-0.0074 (13)
C14	0.055 (2)	0.042 (2)	0.080 (3)	-0.0198 (18)	0.004 (2)	-0.0071 (19)
C15	0.0203 (12)	0.0222 (13)	0.0199 (12)	0.0026 (10)	0.0023 (10)	-0.0008 (10)
C16	0.0245 (13)	0.0198 (13)	0.0304 (14)	0.0001 (11)	0.0061 (11)	0.0016 (11)
C17	0.0225 (13)	0.0259 (14)	0.0398 (16)	0.0013 (11)	0.0091 (12)	-0.0009 (12)
C18	0.0282 (14)	0.0237 (13)	0.0299 (14)	0.0080 (11)	0.0047 (11)	-0.0004 (11)
C19	0.0348 (15)	0.0172 (12)	0.0244 (13)	0.0003 (11)	0.0035 (11)	0.0013 (10)
C20	0.0223 (12)	0.0228 (13)	0.0231 (13)	-0.0025 (10)	0.0018 (10)	0.0013 (10)
C21	0.0212 (12)	0.0168 (12)	0.0234 (12)	0.0043 (10)	0.0057 (10)	0.0053 (10)
C22	0.0278 (14)	0.0239 (13)	0.0269 (14)	-0.0019 (11)	0.0024 (11)	0.0047 (11)
C23	0.0414 (17)	0.0289 (15)	0.0261 (14)	0.0008 (13)	0.0043 (12)	0.0041 (12)
C24	0.0372 (16)	0.0282 (14)	0.0332 (15)	0.0069 (12)	0.0155 (13)	0.0084 (12)
C25	0.0284 (14)	0.0314 (15)	0.0400 (17)	-0.0041 (12)	0.0107 (12)	0.0059 (13)
C26	0.0227 (13)	0.0284 (14)	0.0288 (14)	-0.0011 (11)	0.0049 (11)	0.0037 (11)
Sn2	0.02228 (9)	0.01617 (9)	0.01949 (9)	0.00243 (6)	0.00069 (6)	-0.00094 (6)
S1A	0.0294 (3)	0.0214 (3)	0.0284 (3)	-0.0055 (3)	0.0061 (3)	-0.0041 (2)
S2A	0.0315 (3)	0.0225 (3)	0.0245 (3)	-0.0041 (3)	0.0036 (3)	-0.0031 (2)
S3A	0.0329 (3)	0.0218 (3)	0.0211 (3)	0.0039 (3)	-0.0005 (3)	-0.0011 (2)
S4A	0.0346 (3)	0.0196 (3)	0.0214 (3)	0.0040 (3)	-0.0007 (3)	-0.0014 (2)
N1A	0.0283 (12)	0.0245 (12)	0.0254 (12)	-0.0052 (9)	0.0021 (9)	-0.0036 (9)
N2A	0.0248 (11)	0.0191 (11)	0.0240 (11)	0.0014 (9)	0.0024 (9)	-0.0015 (9)
C1A	0.0246 (13)	0.0213 (13)	0.0233 (13)	-0.0004 (10)	0.0012 (10)	0.0016 (10)
C2A	0.0380 (16)	0.0343 (16)	0.0260 (14)	-0.0104 (13)	0.0057 (12)	-0.0071 (12)

C3A	0.055 (2)	0.0259 (15)	0.0326 (16)	-0.0069 (14)	0.0099 (14)	-0.0063 (12)
C4A	0.051 (2)	0.0301 (16)	0.0383 (17)	-0.0024 (14)	0.0071 (15)	-0.0092 (13)
C5A	0.0270 (14)	0.0298 (14)	0.0267 (14)	-0.0035 (12)	0.0035 (11)	-0.0005 (11)
C6A	0.0364 (17)	0.0426 (19)	0.050 (2)	-0.0105 (15)	-0.0057 (15)	0.0169 (16)
C7A	0.070 (3)	0.093 (3)	0.043 (2)	-0.045 (3)	-0.0174 (19)	0.031 (2)
C8A	0.0227 (12)	0.0203 (13)	0.0228 (12)	0.0001 (10)	0.0028 (10)	-0.0008 (10)
C9A	0.0285 (14)	0.0210 (13)	0.0267 (13)	0.0034 (11)	0.0049 (11)	0.0049 (11)
C10A	0.0296 (14)	0.0238 (13)	0.0260 (13)	0.0057 (11)	0.0004 (11)	-0.0008 (11)
C11A	0.0273 (14)	0.0299 (15)	0.0303 (14)	-0.0005 (12)	0.0014 (11)	-0.0052 (12)
C12A	0.0277 (14)	0.0214 (13)	0.0294 (14)	0.0026 (11)	0.0045 (11)	-0.0054 (11)
C13A	0.0337 (15)	0.0235 (14)	0.0315 (15)	-0.0045 (12)	-0.0012 (12)	-0.0026 (11)
C14A	0.0269 (14)	0.0380 (17)	0.0367 (16)	-0.0042 (13)	-0.0002 (12)	0.0035 (13)
C15A	0.0177 (12)	0.0192 (12)	0.0217 (12)	-0.0005 (10)	0.0004 (9)	0.0022 (10)
C16A	0.0266 (13)	0.0212 (13)	0.0292 (14)	0.0026 (11)	0.0007 (11)	-0.0024 (11)
C17A	0.0232 (13)	0.0206 (13)	0.0388 (16)	0.0042 (11)	0.0010 (11)	0.0038 (11)
C18A	0.0203 (13)	0.0281 (14)	0.0297 (14)	-0.0021 (11)	-0.0012 (11)	0.0095 (11)
C19A	0.0257 (13)	0.0297 (14)	0.0235 (13)	-0.0017 (11)	0.0039 (11)	0.0033 (11)
C20A	0.0204 (12)	0.0216 (13)	0.0253 (13)	0.0019 (10)	0.0059 (10)	0.0009 (10)
C21A	0.0221 (12)	0.0227 (13)	0.0205 (12)	0.0006 (10)	0.0026 (10)	-0.0055 (10)
C22A	0.0244 (13)	0.0266 (14)	0.0275 (14)	0.0021 (11)	0.0035 (11)	-0.0011 (11)
C23A	0.0318 (15)	0.0294 (15)	0.0369 (16)	-0.0001 (12)	0.0105 (12)	0.0019 (12)
C24A	0.0273 (14)	0.0362 (16)	0.0364 (16)	-0.0063 (12)	0.0078 (12)	-0.0089 (13)
C25A	0.0226 (14)	0.0458 (19)	0.0436 (18)	0.0012 (13)	-0.0062 (13)	-0.0012 (15)
C26A	0.0282 (15)	0.0342 (16)	0.0349 (16)	0.0012 (12)	-0.0022 (12)	0.0031 (13)

Geometric parameters (Å, °)

Sn1—C15	2.159 (3)	Sn2—C21A	2.170 (3)
Sn1—C21	2.174 (2)	Sn2—C15A	2.173 (2)
Sn1—S1	2.5501 (6)	Sn2—S1A	2.5585 (7)
Sn1—S3	2.5726 (7)	Sn2—S3A	2.5700 (6)
Sn1—S4	2.6754 (6)	Sn2—S4A	2.6750 (6)
Sn1—S2	2.7393 (7)	Sn2—S2A	2.7664 (7)
S1—C1	1.742 (3)	S1A—C1A	1.740 (3)
S2—C1	1.710 (3)	S2A—C1A	1.704 (3)
S3—C8	1.738 (3)	S3A—C8A	1.733 (3)
S4—C8	1.715 (3)	S4A—C8A	1.716 (3)
N1—C1	1.326 (3)	N1A—C1A	1.328 (4)
N1—C2	1.465 (3)	N1A—C5A	1.477 (4)
N1—C5	1.481 (3)	N1A—C2A	1.480 (3)
N2—C8	1.318 (3)	N2A—C8A	1.327 (3)
N2—C12	1.477 (3)	N2A—C9A	1.465 (3)
N2—C9	1.486 (3)	N2A—C12A	1.466 (3)
C2—C3	1.500 (4)	C2A—C3A	1.496 (5)
C2—H2A	0.9900	C2A—H2A1	0.9900
C2—H2B	0.9900	C2A—H2A2	0.9900
C3—C4	1.317 (4)	C3A—C4A	1.320 (5)
C3—H3	0.9500	C3A—H3A	0.9500

C4—H4A	0.9500	C4A—H4A1	0.9500
C4—H4B	0.9500	C4A—H4A2	0.9500
C5—C6	1.498 (4)	C5A—C6A	1.484 (4)
C5—H5A	0.9900	C5A—H5A1	0.9900
C5—H5B	0.9900	C5A—H5A2	0.9900
C6—C7	1.314 (4)	C6A—C7A	1.317 (6)
C6—H6	0.9500	C6A—H6A	0.9500
C7—H7A	0.9500	C7A—H7A1	0.9500
C7—H7B	0.9500	C7A—H7A2	0.9500
C9—C10	1.496 (4)	C9A—C10A	1.506 (4)
C9—H9A	0.9900	C9A—H9A1	0.9900
C9—H9B	0.9900	C9A—H9A2	0.9900
C10—C11	1.305 (5)	C10A—C11A	1.314 (4)
C10—H10	0.9500	C10A—H10A	0.9500
C11—H11A	0.9500	C11A—H11C	0.9500
C11—H11B	0.9500	C11A—H11D	0.9500
C12—C13	1.496 (5)	C12A—C13A	1.501 (4)
C12—H12A	0.9900	C12A—H12C	0.9900
C12—H12B	0.9900	C12A—H12D	0.9900
C13—C14	1.308 (5)	C13A—C14A	1.311 (4)
C13—H13	0.9500	C13A—H13A	0.9500
C14—H14A	0.9500	C14A—H14C	0.9500
C14—H14B	0.9500	C14A—H14D	0.9500
C15—C20	1.392 (4)	C15A—C16A	1.393 (4)
C15—C16	1.396 (4)	C15A—C20A	1.397 (4)
C16—C17	1.390 (4)	C16A—C17A	1.393 (4)
C16—H16	0.9500	C16A—H16A	0.9500
C17—C18	1.382 (4)	C17A—C18A	1.382 (4)
C17—H17	0.9500	C17A—H17A	0.9500
C18—C19	1.389 (4)	C18A—C19A	1.386 (4)
C18—H18	0.9500	C18A—H18A	0.9500
C19—C20	1.385 (4)	C19A—C20A	1.396 (4)
C19—H19	0.9500	C19A—H19A	0.9500
C20—H20	0.9500	C20A—H20A	0.9500
C21—C26	1.391 (4)	C21A—C22A	1.386 (4)
C21—C22	1.393 (4)	C21A—C26A	1.395 (4)
C22—C23	1.387 (4)	C22A—C23A	1.400 (4)
C22—H22	0.9500	C22A—H22A	0.9500
C23—C24	1.382 (4)	C23A—C24A	1.380 (4)
C23—H23	0.9500	C23A—H23A	0.9500
C24—C25	1.384 (4)	C24A—C25A	1.373 (5)
C24—H24	0.9500	C24A—H24A	0.9500
C25—C26	1.394 (4)	C25A—C26A	1.396 (4)
C25—H25	0.9500	C25A—H25A	0.9500
C26—H26	0.9500	C26A—H26A	0.9500
C15—Sn1—C21	99.84 (9)	C21A—Sn2—C15A	103.34 (9)
C15—Sn1—S1	104.01 (7)	C21A—Sn2—S1A	96.36 (7)

C21—Sn1—S1	92.77 (7)	C15A—Sn2—S1A	101.31 (7)
C15—Sn1—S3	94.80 (7)	C21A—Sn2—S3A	105.20 (7)
C21—Sn1—S3	101.09 (7)	C15A—Sn2—S3A	95.16 (7)
S1—Sn1—S3	154.38 (2)	S1A—Sn2—S3A	149.00 (2)
C15—Sn1—S4	160.59 (7)	C21A—Sn2—S4A	92.74 (7)
C21—Sn1—S4	92.52 (7)	C15A—Sn2—S4A	159.91 (7)
S1—Sn1—S4	90.18 (2)	S1A—Sn2—S4A	88.58 (2)
S3—Sn1—S4	67.97 (2)	S3A—Sn2—S4A	68.69 (2)
C15—Sn1—S2	91.81 (7)	C21A—Sn2—S2A	161.40 (7)
C21—Sn1—S2	159.42 (7)	C15A—Sn2—S2A	88.92 (7)
S1—Sn1—S2	67.824 (19)	S1A—Sn2—S2A	67.18 (2)
S3—Sn1—S2	94.71 (2)	S3A—Sn2—S2A	87.26 (2)
S4—Sn1—S2	81.21 (2)	S4A—Sn2—S2A	78.76 (2)
C1—S1—Sn1	89.92 (8)	C1A—S1A—Sn2	90.15 (9)
C1—S2—Sn1	84.47 (9)	C1A—S2A—Sn2	84.16 (9)
C8—S3—Sn1	89.22 (9)	C8A—S3A—Sn2	87.98 (9)
C8—S4—Sn1	86.37 (9)	C8A—S4A—Sn2	84.96 (9)
C1—N1—C2	122.5 (2)	C1A—N1A—C5A	122.0 (2)
C1—N1—C5	122.6 (2)	C1A—N1A—C2A	123.4 (2)
C2—N1—C5	114.9 (2)	C5A—N1A—C2A	114.5 (2)
C8—N2—C12	122.5 (2)	C8A—N2A—C9A	122.4 (2)
C8—N2—C9	122.6 (2)	C8A—N2A—C12A	122.1 (2)
C12—N2—C9	114.8 (2)	C9A—N2A—C12A	115.5 (2)
N1—C1—S2	123.62 (19)	N1A—C1A—S2A	122.7 (2)
N1—C1—S1	118.58 (19)	N1A—C1A—S1A	119.4 (2)
S2—C1—S1	117.77 (14)	S2A—C1A—S1A	117.94 (16)
N1—C2—C3	112.5 (2)	N1A—C2A—C3A	110.9 (2)
N1—C2—H2A	109.1	N1A—C2A—H2A1	109.5
C3—C2—H2A	109.1	C3A—C2A—H2A1	109.5
N1—C2—H2B	109.1	N1A—C2A—H2A2	109.5
C3—C2—H2B	109.1	C3A—C2A—H2A2	109.5
H2A—C2—H2B	107.8	H2A1—C2A—H2A2	108.1
C4—C3—C2	126.2 (3)	C4A—C3A—C2A	123.2 (3)
C4—C3—H3	116.9	C4A—C3A—H3A	118.4
C2—C3—H3	116.9	C2A—C3A—H3A	118.4
C3—C4—H4A	120.0	C3A—C4A—H4A1	120.0
C3—C4—H4B	120.0	C3A—C4A—H4A2	120.0
H4A—C4—H4B	120.0	H4A1—C4A—H4A2	120.0
N1—C5—C6	111.3 (2)	N1A—C5A—C6A	110.9 (2)
N1—C5—H5A	109.4	N1A—C5A—H5A1	109.5
C6—C5—H5A	109.4	C6A—C5A—H5A1	109.5
N1—C5—H5B	109.4	N1A—C5A—H5A2	109.5
C6—C5—H5B	109.4	C6A—C5A—H5A2	109.5
H5A—C5—H5B	108.0	H5A1—C5A—H5A2	108.0
C7—C6—C5	124.0 (3)	C7A—C6A—C5A	122.9 (4)
C7—C6—H6	118.0	C7A—C6A—H6A	118.5
C5—C6—H6	118.0	C5A—C6A—H6A	118.5
C6—C7—H7A	120.0	C6A—C7A—H7A1	120.0

C6—C7—H7B	120.0	C6A—C7A—H7A2	120.0
H7A—C7—H7B	120.0	H7A1—C7A—H7A2	120.0
N2—C8—S4	122.3 (2)	N2A—C8A—S4A	121.67 (19)
N2—C8—S3	121.3 (2)	N2A—C8A—S3A	120.11 (19)
S4—C8—S3	116.40 (15)	S4A—C8A—S3A	118.21 (15)
N2—C9—C10	109.6 (2)	N2A—C9A—C10A	113.2 (2)
N2—C9—H9A	109.8	N2A—C9A—H9A1	108.9
C10—C9—H9A	109.8	C10A—C9A—H9A1	108.9
N2—C9—H9B	109.8	N2A—C9A—H9A2	108.9
C10—C9—H9B	109.8	C10A—C9A—H9A2	108.9
H9A—C9—H9B	108.2	H9A1—C9A—H9A2	107.7
C11—C10—C9	123.4 (3)	C11A—C10A—C9A	126.1 (3)
C11—C10—H10	118.3	C11A—C10A—H10A	117.0
C9—C10—H10	118.3	C9A—C10A—H10A	117.0
C10—C11—H11A	120.0	C10A—C11A—H11C	120.0
C10—C11—H11B	120.0	C10A—C11A—H11D	120.0
H11A—C11—H11B	120.0	H11C—C11A—H11D	120.0
N2—C12—C13	110.8 (2)	N2A—C12A—C13A	112.3 (2)
N2—C12—H12A	109.5	N2A—C12A—H12C	109.1
C13—C12—H12A	109.5	C13A—C12A—H12C	109.1
N2—C12—H12B	109.5	N2A—C12A—H12D	109.1
C13—C12—H12B	109.5	C13A—C12A—H12D	109.1
H12A—C12—H12B	108.1	H12C—C12A—H12D	107.9
C14—C13—C12	123.8 (3)	C14A—C13A—C12A	126.5 (3)
C14—C13—H13	118.1	C14A—C13A—H13A	116.7
C12—C13—H13	118.1	C12A—C13A—H13A	116.7
C13—C14—H14A	120.0	C13A—C14A—H14C	120.0
C13—C14—H14B	120.0	C13A—C14A—H14D	120.0
H14A—C14—H14B	120.0	H14C—C14A—H14D	120.0
C20—C15—C16	118.6 (2)	C16A—C15A—C20A	118.3 (2)
C20—C15—Sn1	118.07 (19)	C16A—C15A—Sn2	120.81 (19)
C16—C15—Sn1	123.31 (19)	C20A—C15A—Sn2	120.91 (18)
C17—C16—C15	120.3 (2)	C17A—C16A—C15A	121.1 (3)
C17—C16—H16	119.8	C17A—C16A—H16A	119.5
C15—C16—H16	119.8	C15A—C16A—H16A	119.5
C18—C17—C16	120.4 (3)	C18A—C17A—C16A	119.8 (3)
C18—C17—H17	119.8	C18A—C17A—H17A	120.1
C16—C17—H17	119.8	C16A—C17A—H17A	120.1
C19—C18—C17	119.9 (3)	C17A—C18A—C19A	120.3 (2)
C19—C18—H18	120.1	C17A—C18A—H18A	119.9
C17—C18—H18	120.1	C19A—C18A—H18A	119.9
C18—C19—C20	119.7 (2)	C18A—C19A—C20A	119.7 (3)
C18—C19—H19	120.2	C18A—C19A—H19A	120.2
C20—C19—H19	120.2	C20A—C19A—H19A	120.2
C19—C20—C15	121.2 (2)	C15A—C20A—C19A	120.9 (2)
C19—C20—H20	119.4	C15A—C20A—H20A	119.6
C15—C20—H20	119.4	C19A—C20A—H20A	119.6
C26—C21—C22	117.6 (2)	C22A—C21A—C26A	118.0 (3)

C26—C21—Sn1	123.63 (19)	C22A—C21A—Sn2	118.00 (19)
C22—C21—Sn1	118.80 (19)	C26A—C21A—Sn2	124.0 (2)
C23—C22—C21	121.4 (3)	C21A—C22A—C23A	121.3 (3)
C23—C22—H22	119.3	C21A—C22A—H22A	119.4
C21—C22—H22	119.3	C23A—C22A—H22A	119.4
C24—C23—C22	120.2 (3)	C24A—C23A—C22A	119.7 (3)
C24—C23—H23	119.9	C24A—C23A—H23A	120.1
C22—C23—H23	119.9	C22A—C23A—H23A	120.1
C23—C24—C25	119.4 (3)	C25A—C24A—C23A	119.7 (3)
C23—C24—H24	120.3	C25A—C24A—H24A	120.1
C25—C24—H24	120.3	C23A—C24A—H24A	120.1
C24—C25—C26	120.1 (3)	C24A—C25A—C26A	120.7 (3)
C24—C25—H25	120.0	C24A—C25A—H25A	119.7
C26—C25—H25	120.0	C26A—C25A—H25A	119.7
C21—C26—C25	121.3 (3)	C21A—C26A—C25A	120.5 (3)
C21—C26—H26	119.4	C21A—C26A—H26A	119.8
C25—C26—H26	119.4	C25A—C26A—H26A	119.8
C2—N1—C1—S2	0.1 (3)	C5A—N1A—C1A—S2A	4.7 (4)
C5—N1—C1—S2	179.23 (18)	C2A—N1A—C1A—S2A	-175.2 (2)
C2—N1—C1—S1	-178.18 (18)	C5A—N1A—C1A—S1A	-175.4 (2)
C5—N1—C1—S1	1.0 (3)	C2A—N1A—C1A—S1A	4.8 (4)
Sn1—S2—C1—N1	-177.4 (2)	Sn2—S2A—C1A—N1A	172.9 (2)
Sn1—S2—C1—S1	0.89 (13)	Sn2—S2A—C1A—S1A	-7.00 (14)
Sn1—S1—C1—N1	177.43 (19)	Sn2—S1A—C1A—N1A	-172.4 (2)
Sn1—S1—C1—S2	-0.95 (13)	Sn2—S1A—C1A—S2A	7.53 (15)
C1—N1—C2—C3	-95.8 (3)	C1A—N1A—C2A—C3A	-98.2 (3)
C5—N1—C2—C3	85.0 (3)	C5A—N1A—C2A—C3A	81.9 (3)
N1—C2—C3—C4	12.5 (4)	N1A—C2A—C3A—C4A	-105.2 (3)
C1—N1—C5—C6	-91.2 (3)	C1A—N1A—C5A—C6A	-97.9 (3)
C2—N1—C5—C6	88.0 (3)	C2A—N1A—C5A—C6A	82.0 (3)
N1—C5—C6—C7	-122.3 (3)	N1A—C5A—C6A—C7A	-114.6 (4)
C12—N2—C8—S4	179.3 (2)	C9A—N2A—C8A—S4A	2.4 (4)
C9—N2—C8—S4	1.2 (4)	C12A—N2A—C8A—S4A	-173.87 (19)
C12—N2—C8—S3	-0.7 (4)	C9A—N2A—C8A—S3A	-178.66 (19)
C9—N2—C8—S3	-178.79 (19)	C12A—N2A—C8A—S3A	5.1 (3)
Sn1—S4—C8—N2	178.1 (2)	Sn2—S4A—C8A—N2A	175.2 (2)
Sn1—S4—C8—S3	-1.92 (13)	Sn2—S4A—C8A—S3A	-3.74 (14)
Sn1—S3—C8—N2	-178.1 (2)	Sn2—S3A—C8A—N2A	-175.1 (2)
Sn1—S3—C8—S4	1.99 (14)	Sn2—S3A—C8A—S4A	3.88 (15)
C8—N2—C9—C10	101.8 (3)	C8A—N2A—C9A—C10A	88.1 (3)
C12—N2—C9—C10	-76.4 (3)	C12A—N2A—C9A—C10A	-95.3 (3)
N2—C9—C10—C11	105.3 (3)	N2A—C9A—C10A—C11A	-9.9 (4)
C8—N2—C12—C13	104.1 (3)	C8A—N2A—C12A—C13A	90.9 (3)
C9—N2—C12—C13	-77.6 (3)	C9A—N2A—C12A—C13A	-85.6 (3)
N2—C12—C13—C14	110.9 (4)	N2A—C12A—C13A—C14A	-13.3 (4)
C20—C15—C16—C17	-0.4 (4)	C20A—C15A—C16A—C17A	0.9 (4)
Sn1—C15—C16—C17	176.7 (2)	Sn2—C15A—C16A—C17A	-177.9 (2)

C15—C16—C17—C18	0.9 (4)	C15A—C16A—C17A—C18A	-0.7 (4)
C16—C17—C18—C19	-0.7 (4)	C16A—C17A—C18A—C19A	-0.1 (4)
C17—C18—C19—C20	0.0 (4)	C17A—C18A—C19A—C20A	0.7 (4)
C18—C19—C20—C15	0.6 (4)	C16A—C15A—C20A—C19A	-0.3 (4)
C16—C15—C20—C19	-0.4 (4)	Sn2—C15A—C20A—C19A	178.47 (19)
Sn1—C15—C20—C19	-177.60 (19)	C18A—C19A—C20A—C15A	-0.5 (4)
C26—C21—C22—C23	-0.7 (4)	C26A—C21A—C22A—C23A	-1.2 (4)
Sn1—C21—C22—C23	180.0 (2)	Sn2—C21A—C22A—C23A	179.5 (2)
C21—C22—C23—C24	-0.2 (4)	C21A—C22A—C23A—C24A	1.1 (4)
C22—C23—C24—C25	0.5 (4)	C22A—C23A—C24A—C25A	-0.4 (4)
C23—C24—C25—C26	0.1 (4)	C23A—C24A—C25A—C26A	-0.1 (5)
C22—C21—C26—C25	1.2 (4)	C22A—C21A—C26A—C25A	0.7 (4)
Sn1—C21—C26—C25	-179.5 (2)	Sn2—C21A—C26A—C25A	180.0 (2)
C24—C25—C26—C21	-0.9 (4)	C24A—C25A—C26A—C21A	-0.1 (5)

Hydrogen-bond geometry (\AA , $^\circ$)

*Cg*1 and *Cg*2 are the centroids of the (C15A—C20A) and (C21A—C26A) rings, respectively.

<i>D</i> —H... <i>A</i>	<i>D</i> —H	H... <i>A</i>	<i>D</i> ... <i>A</i>	<i>D</i> —H... <i>A</i>
C7—H7A... <i>Cg</i> 1 ⁱ	0.95	2.83	3.774 (3)	172
C7—H7B... <i>Cg</i> 2 ⁱⁱ	0.95	2.92	3.582 (3)	128

Symmetry codes: (i) $-x+2, -y+1, -z+1$; (ii) $-x+1, -y+1, -z+1$.